

WEATHERSMART

NEWS

Scientific meteorological and climatological
news from the South African Weather Service

October 2021

**New regional Weather and
Climate Summaries: Gauteng
Province**

**Adverse winter weather over the
Eastern Cape: 1 to 3 June 2021**

**Devastating fires on Table
Mountain at the University of
Cape Town: 18 to 20 April 2021**

**Pilot Operational Rip Risk
Warning System**



**South African
Weather Service**

WEATHERSMART

NEWS Scientific meteorological and climatological news from the South African Weather Service

Impact-Based Severe Weather Warning System

WHAT IS IMPACT-BASED FORECASTING?

Severe weather is a regular occurrence across South Africa which often negatively affects humans. Due to the vast distribution of vulnerabilities across the country, the same weather hazard can result in different impacts in two areas, depending on the specific vulnerability of the area.

Impact-Based warnings combine the level of impact the hazardous weather conditions expected with the level of likelihood of those impacts taking place

Moving from

What the weather will be:
(Meteorological thresholds)
- 50mm in 24 hours - 35 knot winds

To

What the weather will do:
(Impact Warnings)
- Roads flooded - Communities cut off

Date of issue:
October 2021

Frequency:
Bi-annual

ISSN:
2414-8644

Compiler and editor: Hannelee Doubell

Publisher:
South African Weather Service
Address:
Eco Glades Block 1B, Eco Park,
Corner Olievenhoutbosch and
Ribbon Grass Streets,
Centurion, 0157

TABLE OF CONTENTS

Foreword by the Chief Executive Officer, Mr Ishaam Abader.....	2
New Regional Weather and Climate Summaries: Gauteng Province <i>by Andries Kruger</i>	3
Presenting the South African Weather Service (SAWS) Lightning Detection Network and related services to the South African Institute of Electrical Engineering (SAIEE) Lightning Chapter (LC) <i>by Rydall Jardine and Morné Gijben</i>	9
Adverse winter weather over the Eastern Cape – 1 to 3 June 2021 <i>by Ayabonga Tshungwana and Nompumelelo Kleinboo</i>	12
The Performance Assessment of Six Global Horizontal Irradiance Clear Sky Models in Six Climatological Regions in South Africa <i>by Brighton Mabasa, Meena D. Lysko, Henerica Tazvinga, Nosipho Zwane and Sabata J. Moloji</i>	18
The Ångström–Prescott Regression Coefficients for Six Climatic Zones in South Africa <i>by Brighton Mabasa, Meena D. Lysko, Henerica Tazvinga, Sophie T. Mulaudzi, Nosipho Zwane and Sabata J. Moloji</i>	25
Devastating fires on Table Mountain at the University of Cape Town: 18 to 20 April 2021 <i>by Ntshalle Stella Nake, Cape Town Weather Office</i>	32
Pilot Operational Rip Risk Warning System <i>by Carla-Louise Ramjukadh</i>	38
Meet the Authors.....	44

Foreword by the Chief Executive Officer

As CEO of this prestigious and internationally recognised entity since April 2021, I am delighted to welcome our readers to the Weathersmart News of October 2021. This publication contains scientific weather news and is published twice a year to share some of our scientific work with the public.

This edition covers the new Regional Weather and Climate Summaries for Gauteng, developed by our scientists in our Climate Service department. The series provides a broad overview of the climate and weather of different regions in South Africa, especially those regions that are of relative greater economic and/or demographic significance in the country.

The article on the South African Weather Service (SAWS) Lightning Detection Network and related services to the South African Institute of Electrical Engineering (SAIEE) Lightning Chapter (LC), which demonstrates the value of this system to weather sensitive energy industries.

From 1 to 3 June 2021, adverse weather conditions that occurred over the Eastern Cape, brought welcome relief to some areas in the region. A ridging high-pressure system, coupled with a cut-off low (COL) over the eastern parts of the country formed the dominant systems. These two systems resulted in showers and thundershowers over the southern and eastern parts of the Eastern Cape and very cold conditions were experienced. SAWS issued warnings, including for snowfall, for the system which had a likelihood of significant impacts. The way in which this system was forecast and warnings issued demonstrates the importance of local forecasting skills to accurately forecast impacts related to expected adverse weather.

For those interested in the deeper levels of scientific research by our scientists, two scientific articles on *The Performance Assessment of Six Global Horizontal Irradiance Clear Sky Models in Six Climatological Regions in South Africa* and *The Ångström–Prescott Regression Coefficients for Six Climatic Zones in South Africa* that

were published in *Multidisciplinary Digital Publishing Institute (MDPI) Energies* should satisfy their curiosity in this regard.

An article on the devastating fires on Table Mountain and at the University of Cape Town talks to the bush fire disaster that occurred from 18 to 20 April 2021, causing huge damage to some historical buildings at the University of Cape Town, among other damage.

We end this edition with a very interesting article on a project in its pilot phase which seeks to operationalise a Rip Risk Warning System in South Africa. As rip currents are currently not being operationally forecast and warned for in South Africa, and more than 30 drownings occur annually due to rip currents, work in this regard is of future significance to protect the lives of beach goers, especially during the holiday seasons.

I would like to congratulate our scientific personnel for their contributions to the WeatherSMART news of October 2021 and hope that the content is enjoyed by a wide audience of weather enthusiasts, scholars and researchers.

Ishaam Abader
October 2021



New Regional Weather and Climate Summaries: Gauteng Province

by Andries Kruger

Department: Climate Service

Introduction

The Climate Service department of the South African Weather Service (SAWS) recently released the first publication in a new series of *Regional Climate and Weather Summaries* (<https://www.weathersa.co.za/home/regionalweatherclimate>), which focuses on the Gauteng province. The series provides a broad overview of the climate and weather of different regions in South Africa, especially those regions that are of relative greater economic and/or demographic significance in the country. The first in the series focuses on the Gauteng province as it is the most populous of the nine provinces of South Africa and the main economic hub of the country. The publication is comprehensive and consists of 53 figures and graphs, 15 tables and comprises almost 60 pages. This article presents a summary of the contents of the publication and those aspects of the weather and climate which, in general, can be expected to be included in forthcoming publications for other regions.

During the planning phases of the series a thorough needs analysis was done to explore the possible content to include in the publication. This process involved mainly the examination of available regional climate publications internationally, thereby obtaining ideas and approaches which will be useful in the development of the format of the publication. All possible countries which could have comprehensible information language-wise, were investigated. However, the focus remained on the publications which are produced by National Meteorological and Hydrological Services who, in most instances, have access to most climate data in a particular country. In conclusion the envisaged content was divided into additional information and alternative formats to those presented in the current SAWS general climate publications, which could possibly be considered for the publication. In addition, it was also considered that these publications should present baseline information on the weather and climate of a particular region, to support the information already available from the information portal of the National Framework for Climate Services (NFCS).

Topics covered

Topics for inclusion in the series broadly are similar to those included in the series of SAWS publications that provide overviews of the South African climate and are mainly divided into a range of common weather parameters. The first of these publications was completed in 2002 on surface winds and covered the whole country. The publications that followed were developed according to the same principle, with the last one, published in 2008, on surface temperature. The above publication series covered their individual topics in fair detail and it was envisaged in the planning phase that the regional climate publications will at least cover most of the relevant aspects of the climate included in the last series. In addition a range of additional content that could potentially be included in the new publication was identified from the desktop analysis of international publications. Thereafter, the proposed content was arranged into a coherent structure.

Content

The content of the publication follows a logical structure, with an introduction explaining the factors that control the region's climate and therefore the general climate in relation to other climate regimes in South Africa. This is followed by detailed chapters about the main climate parameters in which the envisaged audience will mostly be interested in. A conclusion chapter discusses the impact of climate change on the region through evidence of observed climate change and its impacts.

Introduction

The factors influencing the weather and climate are presented, how the province is situated in relation to the diverse climate regions of South Africa and the differences in weather experienced on a seasonal basis. For example, according to the Köppen Climatic Classification System, Gauteng is situated in the interior in the eastern half of South Africa, experiencing relative moderate weather and climate conditions, classified as Cwa (summer rain with hot summers) in the north and

Cwb (summer rain with cool summers) in the south.. A more detailed classification system developed by SAWS places Gauteng mostly in the Moist Highveld Grassland region and the Central Bushveld in the north, as presented in Figure 1.

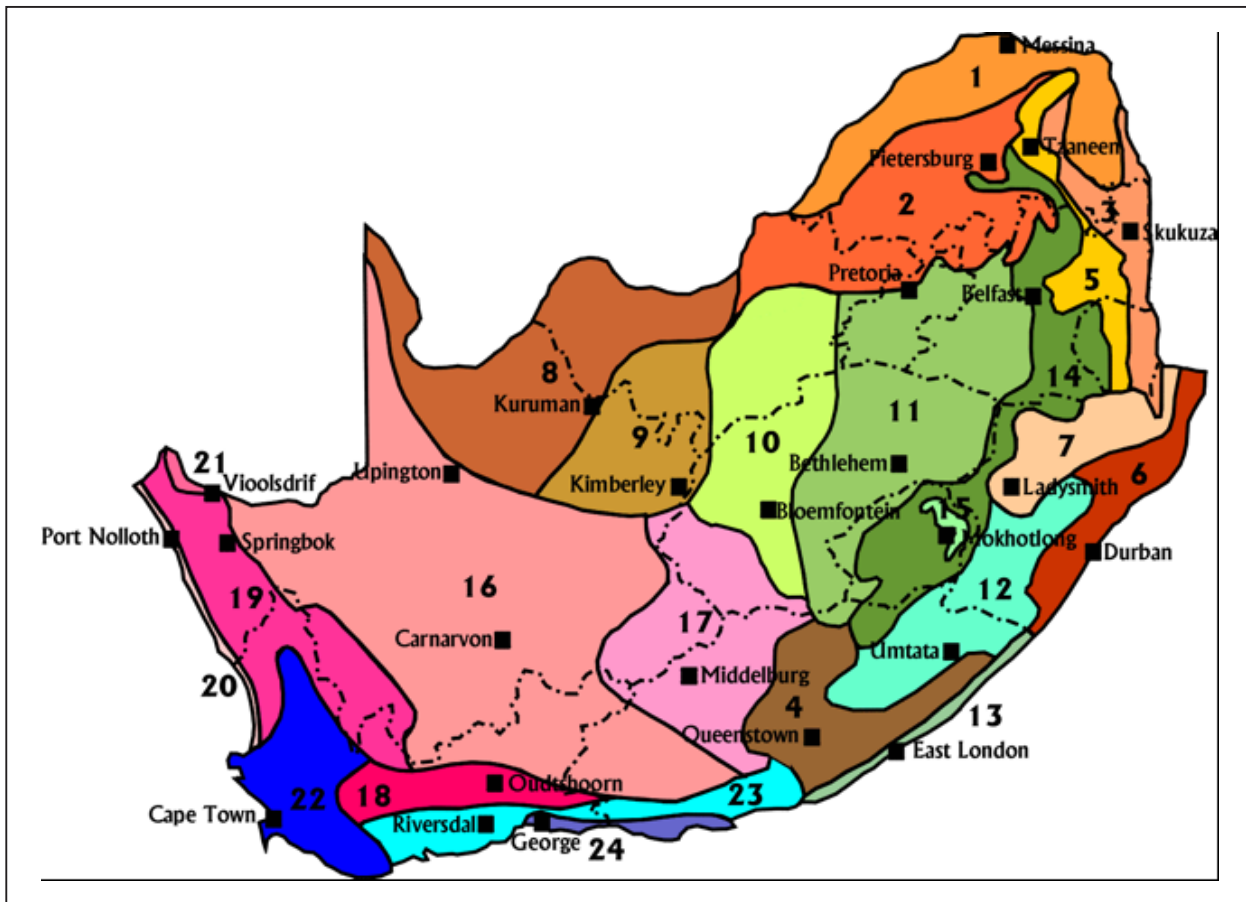


Figure 1: The Climatic Regions of South Africa: 1. Northern Arid Bushveld 2. Central Bushveld 3. Lowveld Bushveld 4. South-Eastern Thornveld 5. Lowveld Mountain Bushveld 6. Eastern Coastal Bushveld 7. KwaZulu-Natal Central Bushveld 8. Kalahari Bushveld 9. Kalahari Hardveld Bushveld 10. Dry Highveld Grassland 11. Moist Highveld Grassland 12. Eastern Grassland 13. South-Eastern Coast Grassland 14. Eastern Mountain Grassland 15. Alpine Heathland 16. Great and Upper Karoo 17. Eastern Karoo 18. Little Karoo 19. Western Karoo 20. West Coast 21. North-Western Desert 22. Southern Cape Forest 23. South-Western Cape 24. Southern Cape.

Wind

The climate controls described in the previous section have a direct influence on the general wind field over the province. The high-resolution wind resource map developed by the Wind Atlas for South Africa project (WASA: www.wasaproject.info) is included and sheds more light on the spatial variation of the average wind speed in the province. In the north-west winds tend to be lightest, while in the south-west the winds are the strongest. The mean wind speed tends to follow the topography of the province with the northern parts generally lower than the south, as presented in Figure 2.

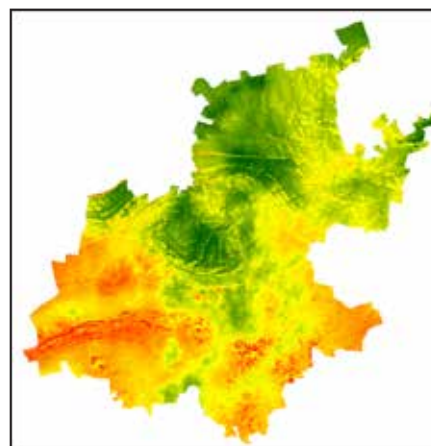


Figure 2: WASA High Resolution Wind Resource Map for Gauteng province. Mean wind speed (m/s) at 50 m above ground with lower wind speeds in green (< 3 m/s) and higher wind speeds in red (> 7 m/s) (www.wasaproject.info).

Also discussed are the annual and diurnal variation of wind speed and strong winds of short duration, the causes thereof and the likelihood and documented occurrences of tornadoes. For example, Figure 3 presents the 5-minute measurements of wind gust (m/s), wind direction (degrees), surface temperature (°C), rainfall (mm) and surface pressure (hPa) at the Irene weather office on 30 December 2017, when one of the strongest wind gusts was recorded at the station.

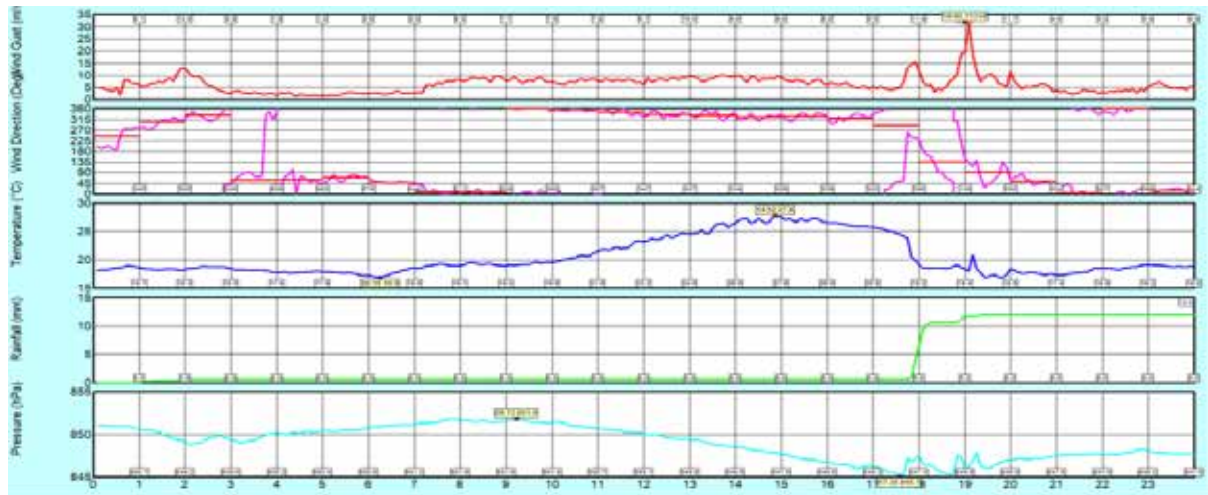


Figure 3: 5-minute measurements of wind gust (m/s), wind direction (degrees), surface temperature (°C), rainfall (mm) and surface pressure (hPa) at the Irene Weather Office on 30 December 2017.

Surface temperature

The average surface temperature is governed by the general circulation patterns and topography, amongst others. The mean seasonal temperatures as well as minimum and maximum temperature, are presented in map format, from which it can be deduced that the northern parts of the province generally experience higher temperatures than the south (this feature of surface temperature is related to the topography, where lower (higher) elevations experience higher (lower) temperatures). As an example, Figure 4 presents the mean winter (JJA) minimum temperature (°C) over Gauteng, based on topography and data for the period 1991 – 2020.

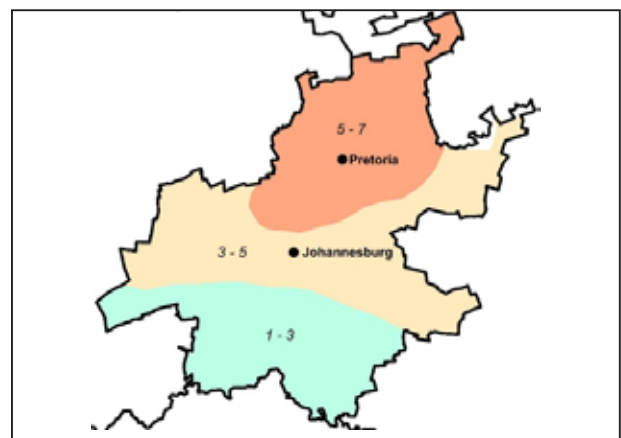


Figure 4: Mean winter (JJA) minimum temperature (°C) over Gauteng, based on topography and data for the period 1991 – 2020.

Extreme temperatures and the synoptic conditions that occurred during the recording of all-time maximums and minimums are discussed in detail. Figure 5 presents the highest ever temperature recorded at the UNISA automatic weather station.

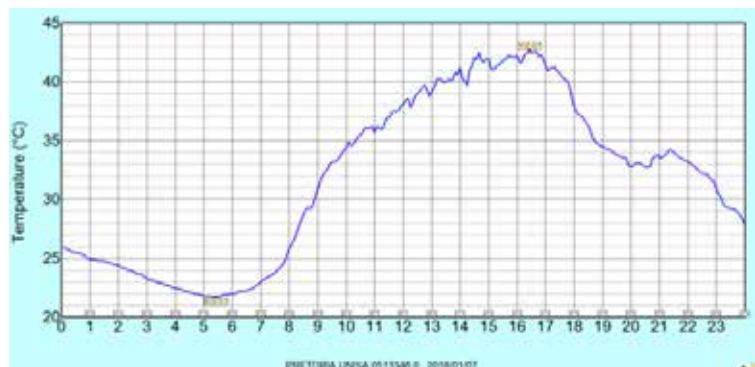


Figure 5: 5-minute graph of surface temperatures measured on 7 January 2016 at Pretoria UNISA automatic weather station.

In addition, frequency tables of temperature in specified ranges of 5 °C, at specified times for some weather stations in the province, are included and the topics of apparent temperature and the likelihood of frost are discussed.

Sunshine and Cloudiness

Gauteng receives a relative high amount of sunshine, compared to the rest of the world, but not particularly so for South Africa. The province receives just more than 70% of the maximum possible sunshine, which equates to an annual average of more than 8 hours of sunshine per day. In comparison, the western interior receives more than 80% and the east coast mostly below 55%. This spatial variation of mean sunshine received over the country is presented in map format, with additional monthly maps. An analysis of daily sunshine shows that, on an annual basis, Gauteng experiences fewer than 10 overcast days, in the region of 20 cloudy days, just over 300 sunny days and more than 150 fine days, with the last-mentioned mostly occurring in the winter and early spring. The monthly variation of the days is presented graphically in Figure 6.

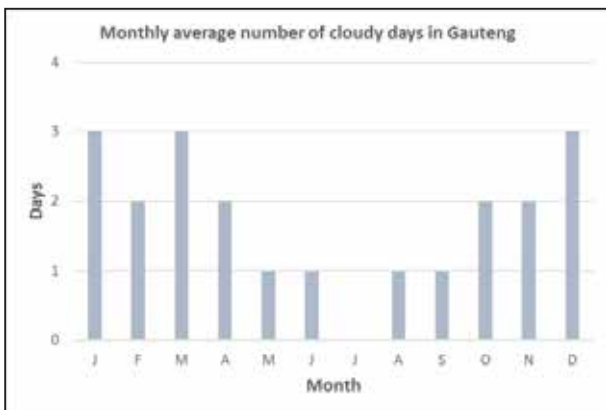


Figure 6: Average number of cloudy days in Gauteng per month (1991 – 2020).

With the drive from fossil fuels to renewable energy sources, wind and solar energy have become increasingly important for our future energy needs. Gauteng’s position in the north of South Africa restricts the local exploitation of wind for energy generation, compared to the relatively windy south. Solar energy is a very viable source of energy in the province. Solar energy resource information is widely available, particularly in atlas format. Developers and users of solar energy are mostly interested in the direct normal irradiation, global horizontal irradiation and resultant power potential. Atlases with this information are readily

available from the Global Solar Atlas web portal (<https://globalsolaratlas.info/>), endorsed by the World Bank, and presented in the publication.

Precipitation

As an introduction, the annual and seasonal distribution of rainfall is presented in map format (see Figure 7).

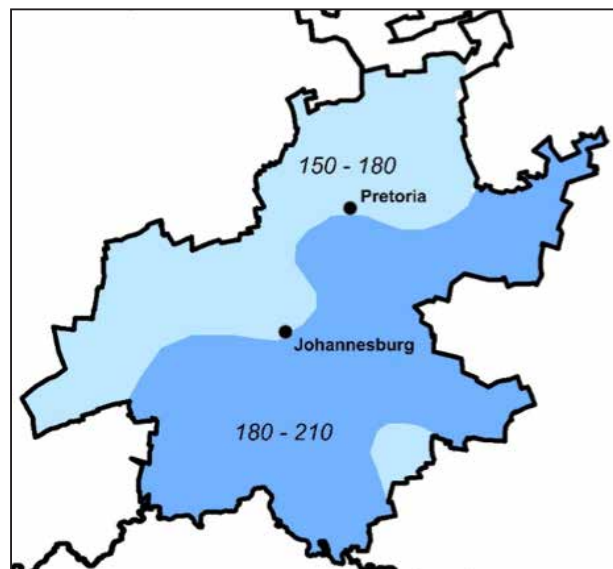


Figure 7: Mean spring (SON) rainfall (mm) based on topography and data over the period 1991 – 2020.

The frequencies of wet and dry years, the Standardised Precipitation Index (SPI) and the Standardised Precipitation Evaporation Index (SPEI) and trends thereof over the long-term are discussed (see Figure 8). In addition, the role of El Niño/South Oscillation on the rainfall over the province is discussed.

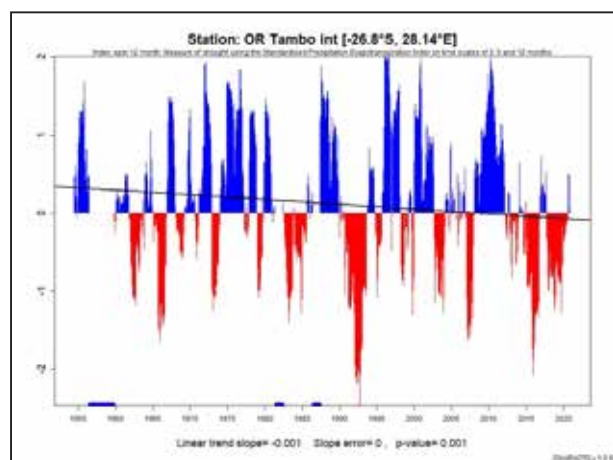


Figure 8: 12-month SPEI for OR Tambo International Airport (1953 – Jan 2021).

Following on the above the average number of rainy days per month, above-specific thresholds are presented as well as the likelihood of rainfall during specific hours of the day in the different seasons.

Floods are usually caused by persistent rainfall of various intensity over a prolonged period or a lot of rainfall over a short period. In Gauteng floods are usually caused by the latter. The automatic weather station technology that SAWS utilises provides the rainfall amounts to a frequency of five minutes. The frequencies with which the rainfall exceeded 5 mm, 10 mm and 15 mm within a five-minute period over the 1991 – 2020 period were analysed and are presented in tabular format. In addition, the mean monthly frequencies of reported heavy precipitation events are presented.

Climate change

Due to the increase in greenhouse gases since the Industrial Revolution, of which carbon dioxide is the most important, the atmosphere has been gradually warming over a long period of time. The increase in atmospheric warming can be traced back for centuries and has increased over the last 100 years by about 1 °C. This warming of the atmosphere obviously causes warmer surface temperatures in general but also changes other atmospheric properties, e.g. changes in the general circulation and the likelihood of climate extremes, amongst others. The change in the global climate is expected to accelerate and there are already clear signals that this is happening. The long-term changes in the climate and extreme weather occurrences are discussed. For example, Figure 9 presents the annual average surface temperature deviation at OR Tambo International Airport for the period 1955 to 2020, which clearly indicates a warming trend close to 0,2 °C per decade over the analysis period.

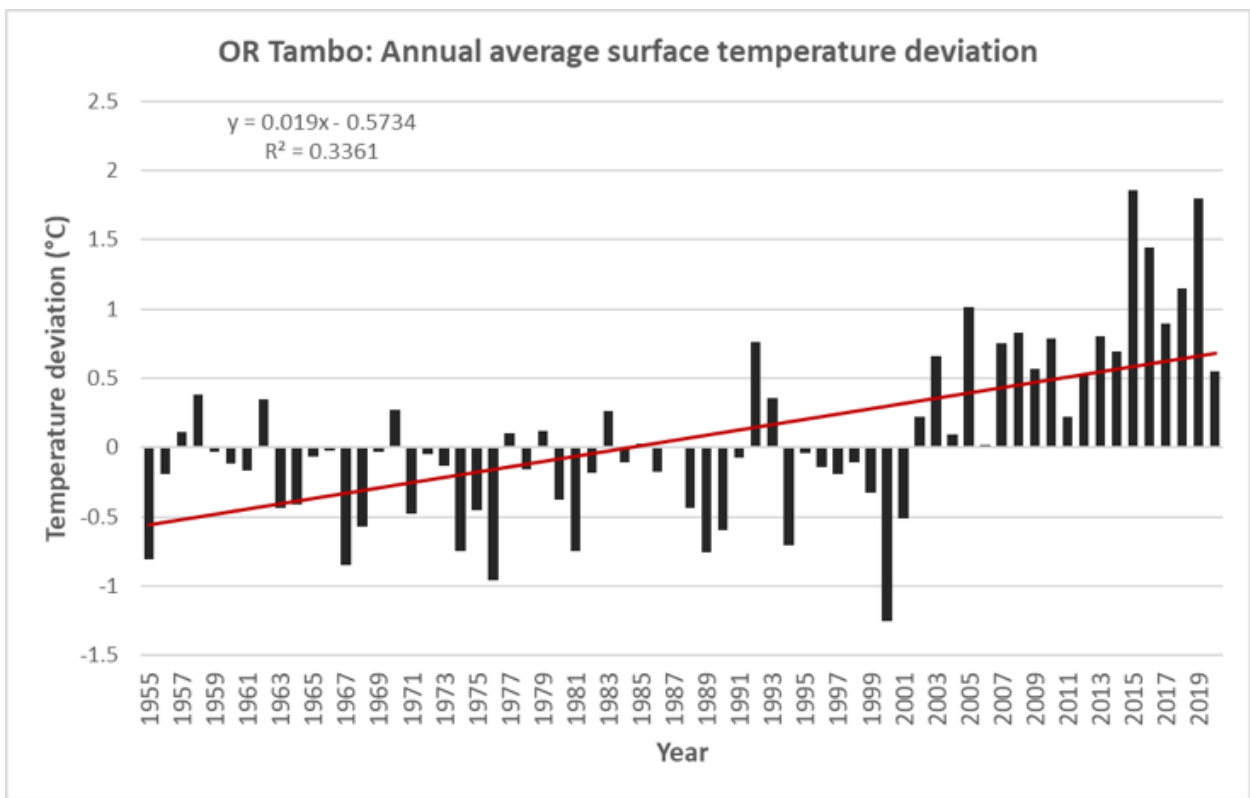


Figure 9: Annual average surface temperature deviations at OR Tambo International Airport for the period 1955 to 2020 (base period: 1981 – 2010).

As mentioned, climate change is mostly experienced through increased occurrences of anomalous weather events, e.g. very hot days. The trends in the frequencies of extreme events in the province, in comparison to the rest of the country, are discussed.

An assessment of the frequencies of specific weather events (e.g. large hail or floods) over a long period of time can only be done through an analysis of media reports. SAWS produces the CAELUM publication which provides a geocoded list of significant weather events which were reported in South Africa from 1647. It should be noted that such reports are highly dependent on demographics and population density, where a relatively high population density and the presence of the print media and other documenters makes the documentation of significant weather events more probable. Also, the amount of damage and/ or loss of life that a significant

weather event causes also influences its coverage in the media. In spite of the above shortcomings it is important to analyse these reports to assess the most prevalent events and whether a trend in these events can be discerned. It is shown that in Gauteng, most significant weather reports are on floods, hail and strong wind and their related impacts. The annual number of reports on floods, hail and strong wind were analysed over the period 1961 – 2020 and presented graphically. For all these types of events increasing trends are noticeable, as shown for heavy rain and flooding in Figure 10. These trends can be ascribed to an increase in population density (and therefore more people are affected and can report events) as well as a probable increase in severe weather events, e.g. stronger thunderstorms. The last-mentioned hypothesis can be linked to the results presented in the previous section, which indicates an intensification in rainfall events over the province.

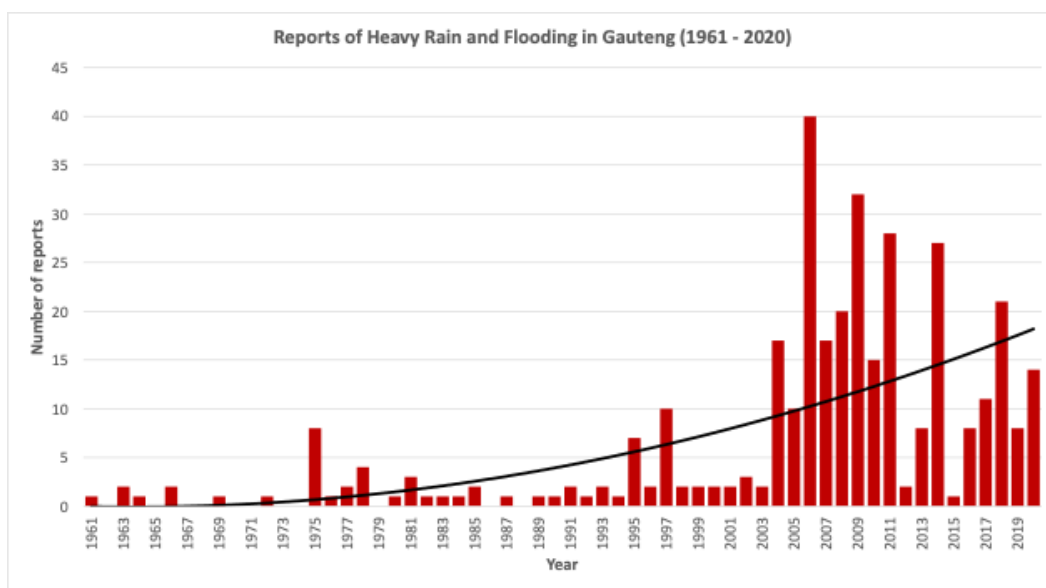


Figure 10: The annual number of reports on heavy rain and flooding in the Gauteng province over the period 1961 – 2020.

Way forward

It is envisaged that the regional weather and climate series will continue in the 2021/22 financial year, with the next publication that will focus on the South-Western Cape. For each of these publications, special emphasis will be placed on the weather and climate that significantly impact the region. For example, the South-Western Cape publication will include a section on veld fires, which is a regular occurrence in the winter rainfall regions of South Africa. This series is envisaged to be regarded as the reference point of climate information for the country and will be disseminated as a SAWS public good service through the National Framework for Climate Services.

Presenting the South African Weather Service (SAWS) Lightning Detection Network and related services to the South African Institute of Electrical Engineering (SAIEE) Lightning Chapter (LC)

by Rydall Jardine and Morné Gijben

The South African Weather Service (SAWS) Lightning Detection Network (LDN) was initiated through a stakeholder engagement process with Eskom in 2005 and consists of sensors designed to detect Cloud-to-Ground (CG) lightning activity with great accuracy. CG lightning, as the name suggests, is the lightning that occurs between the cloud and the ground and is also the lightning that affects us. Although designed for detecting CG lightning, the sensors in the network are also capable of detecting a portion of cloud lightning, which is the lightning occurring inside clouds.

The existing network has 24 SAWS-owned sensors and one owned by the Eswatini Meteorological Service. Currently, 17 of the SAWS-owned sensors and the Eswatini-owned sensor are the Vaisala LS-7000 version. Another four SAWS-owned sensors are the Vaisala LS-7001 version, while three of the SAWS-owned sensors were upgraded to the Vaisala LS-7002 version in 2020, with further upgrades planned over the next three years. SAWS has also upgraded its Total Lightning Processor (TLP) software in 2019 with enhanced algorithms. Figure 1 shows the existing positions of the LDN sensors across South Africa.



Figure 1: Existing positions of LDN sensors across South Africa.

The network coverage maps in Figure 2 provide an indication of the area being serviced, with an indication of the projected Detection Efficiency (DE) and the Location Accuracy (LA). The DE represents the percentage of all lightning flashes that can be detected (90% means

that more than 90% of CG lightning flashes can be detected), while the Location Accuracy (LA) refers to the distance in which a detected lightning stroke is placed with regard to the actual lightning stroke.).

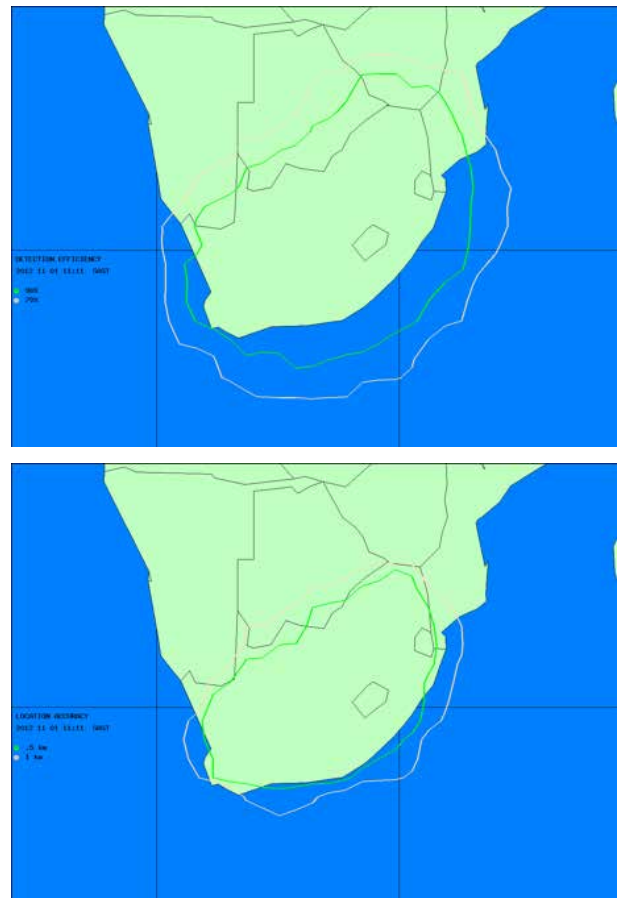


Figure 2: Detection Efficiency (left) and Location Accuracy (right) projections of the network.

From a lightning data application perspective, real-time observations of lightning across South Africa play an important role in the monitoring and nowcasting of thunderstorms. Since all thunderstorms contain lightning, real-time data is used to monitor the position, movement and how electrically active a storm is. This information is also used to supplement other observation platforms such as weather radar and satellite observations and is used to assist with storm tracking and nowcasts. Lightning information is very useful in areas not covered by radars or when a radar is not available. In such cases lightning tracking can be utilised.

As per the example below, the current storm cell tracks can be provided within the redline outlay and the movement of the storm cells can be nowcasted for the next 30 minutes (blue-lined outlay) and 60 minutes (green-lined outlay). This is very helpful for nowcasting the expected movement of storms in the next hour whenever radar is not available or to supplement radar observations and nowcasts.

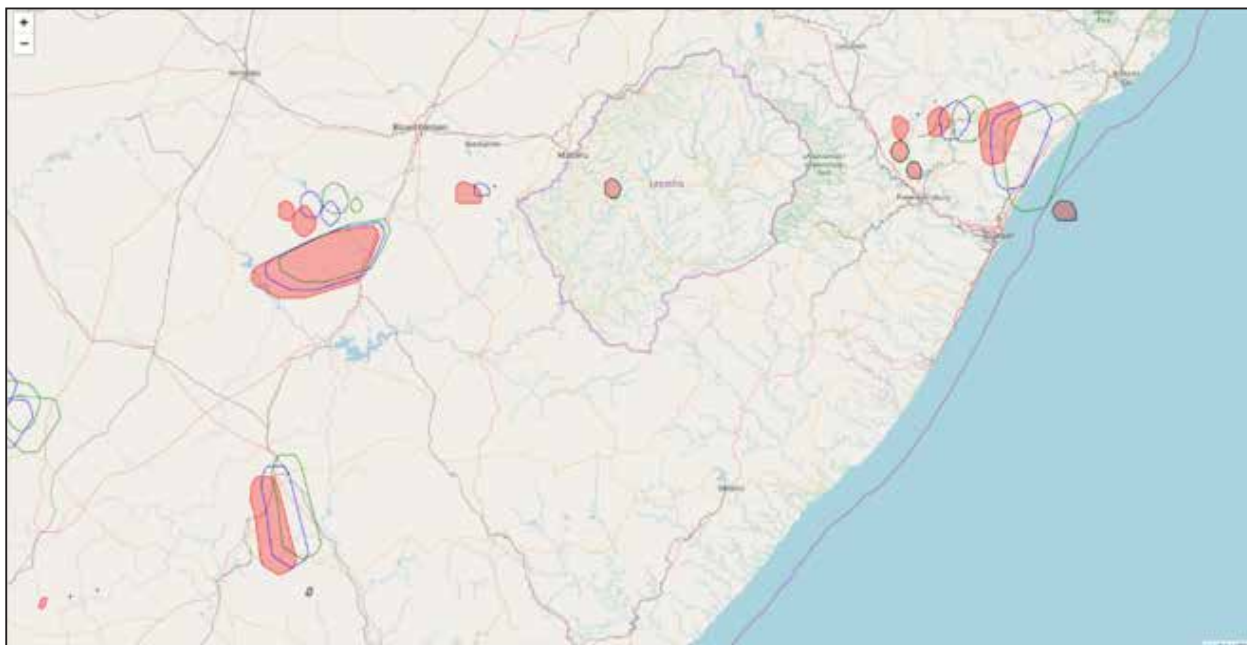


Figure 3: The tracking and nowcasting of lightning cells.

Historical lightning information from the SAWS LDN has been available since 2006 and is useful for many applications. One such an example is for the development of lightning prediction models. Historical lightning observations were used to train a model by using machine learning techniques to provide a daily probability forecast for lightning from Numerical Weather Prediction (NWP) model parameters. This model forecast is available early in the morning and provides a probability outlook of where lightning could be expected during the day. Figure 4 is an example for 20 December 2013, where the model on the left shows the forecast for the day, while on the right the actual observed lightning activity for this day is shown.

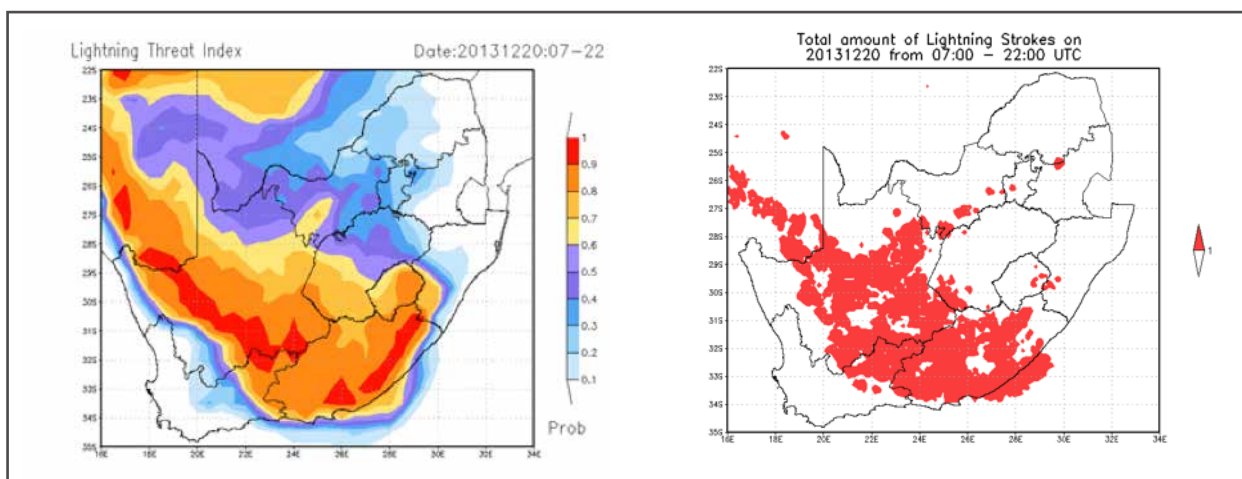


Figure 4: The model-based lightning probability forecast (left) and the actual observed lightning (right).

The historical lightning data is utilised for climatological purposes, where various maps such as the Average Lightning Ground Flash Density, Median Peak Kiloampere, Average Flash Multiplicity (number of strokes in a flash) and several lightning risk maps are produced and updated annually. This information is extremely useful for climatological studies as well as for design and planning purposes by many industries. Figure 5 shows examples of typical lightning climatology maps.

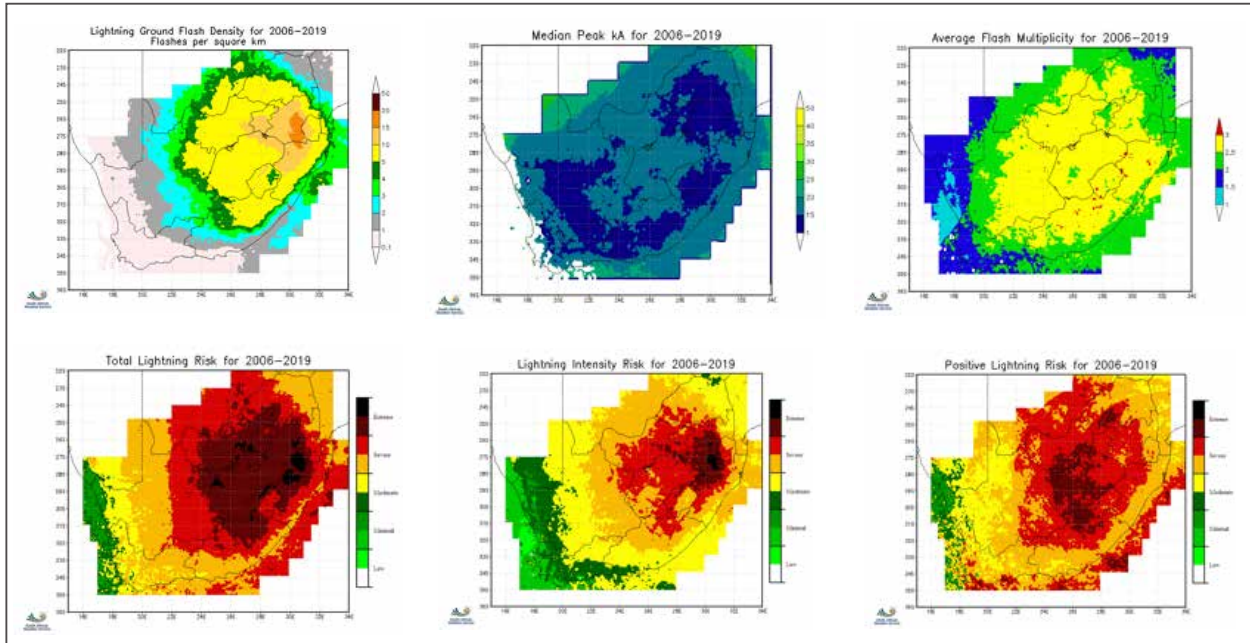


Figure 5: Typical lightning climatology maps produced by SAWS and updated annually.

With a diminishing Government Grant, SAWS implemented a cost recovery strategy across its infrastructure technology applications. Eskom utilises lightning data for overhead line design (route selection), performance analysis during design, asset management of existing lines and fault correlation. The aviation industry requires the lightning activity in the vicinity of an airport in order to stop operations during storms. The insurance industry receives many lightning-related claims and SAWS' lightning data is used extensively for claim verification purposes. The graph in Figure 6 (left) provides a typical indication of the number of lightning activity enquiries from the insurance sector as indicated by the blue line, in relation to all queries received from the insurance sector as indicated by the orange line. This shows lightning enquiries form a large component of insurance-related queries received by SAWS. Figure 6 (centre) represents an Overhead High Voltage Cable path from a power utility such as Eskom, and the spatially-correlated lightning occurring in a buffer zone around the line. Figure 6 (right) represents a lightning alert system over O.R. Tambo International Airport where activities in and around airport are broken into 5 km rings expanding to 15 km around the airport.



Figure 6: The typical amount of lightning (blue line) and total number (orange line) of queries received from the insurance sector (left), example of correlated lightning to power lines (centre) and a lightning alert system over O.R. Tambo International airport (right).

Adverse winter weather over the Eastern Cape: 1 to 3 June 2021

by Ayabonga Tshungwana and Nompumelelo Kleinbooi

From 1 to 3 June 2021, adverse weather conditions that occurred over the Eastern Cape, brought welcome relief to some areas in the region. A ridging high-pressure system, coupled with a cut-off low (COL) over the eastern parts of the country formed the dominant systems, as seen in Figure 1. These two systems were expected to result in showers and thundershowers over the southern and eastern parts of the province from Tuesday, 1 June 2021, with good chances for showers along the Wild Coast and adjacent interior. Further, these systems were advecting cold air over the province, with very cold conditions over the north-eastern high ground where snowfalls were expected.

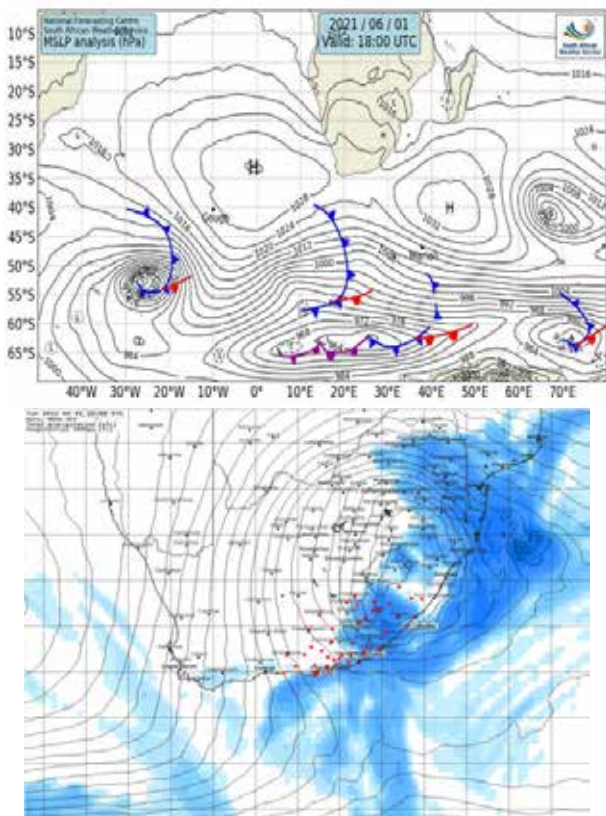


Figure 1: Dominant systems over South Africa on 1 June 2021

Individual parameters

Rainfall

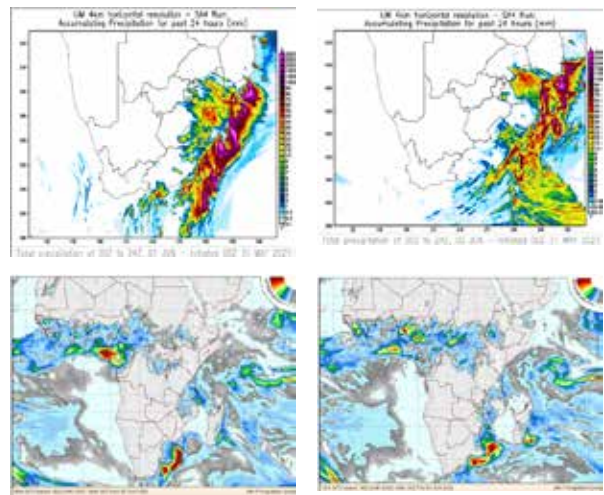


Figure 2: Model outputs showing expected precipitation for 01 June and 02 June 2021

Significant amounts of rainfall were expected to result in flooding of roads and settlements, low-lying areas as well as bridges. Traffic disruptions, damage to property and infrastructure and isolated incidents of rockfalls were expected over the OR Tambo District Municipality (DM), Alfred Nzo DM, places over Amathole DM and the eastern parts of Chris Hani DM. The expected rainfall amounts can be seen in Figure 3 below.

Table 1: Observed rainfall amounts for 1 to 3 June 2021 in places over the eastern parts of the province.

Station	Observed rainfall amounts (mm)			
	1 June	2 June	3 June	Total
Coffee Bay	67.4	81.4	15.4	164.2
Port Edward	78.2	57.6	22	157.8
Mthatha	17.4	30.8	1.8	50
Barkley East	2.4	0.8	24	27.2
Elliot	13.6	6.8	3.2	23.6

Snowfall

Low freezing levels were expected over the north-eastern high ground, where snowfall was expected. Accumulations of 0.5 to 5 cm were expected, with 6 to 15 cm over the Sakhisizwe Local Municipality (LM), Elundini LM and Matatiele LM as shown in Figure 3.

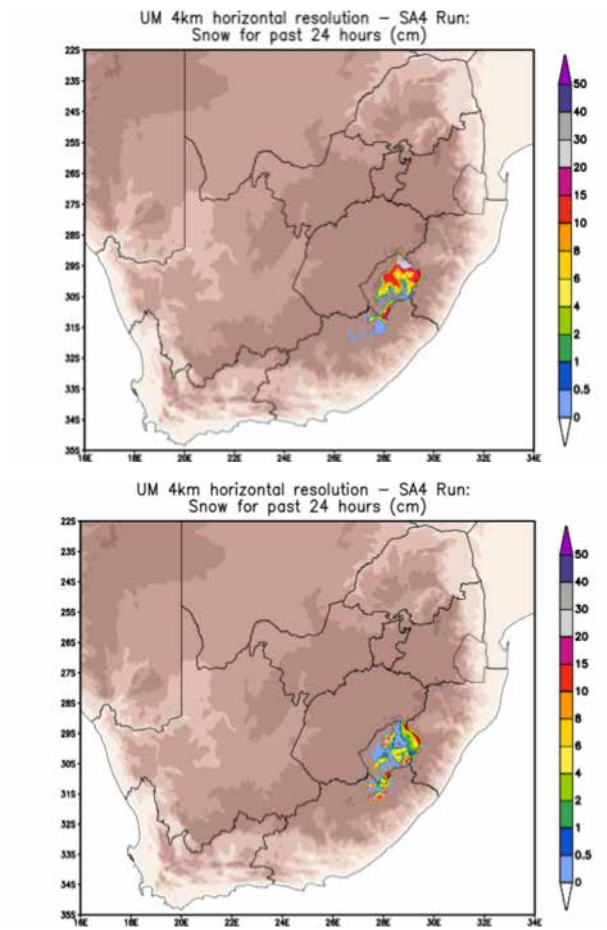


Figure 3: Expected snow accumulations over the north eastern high ground from 1 June to 2 June 2021 (UM SA4km)

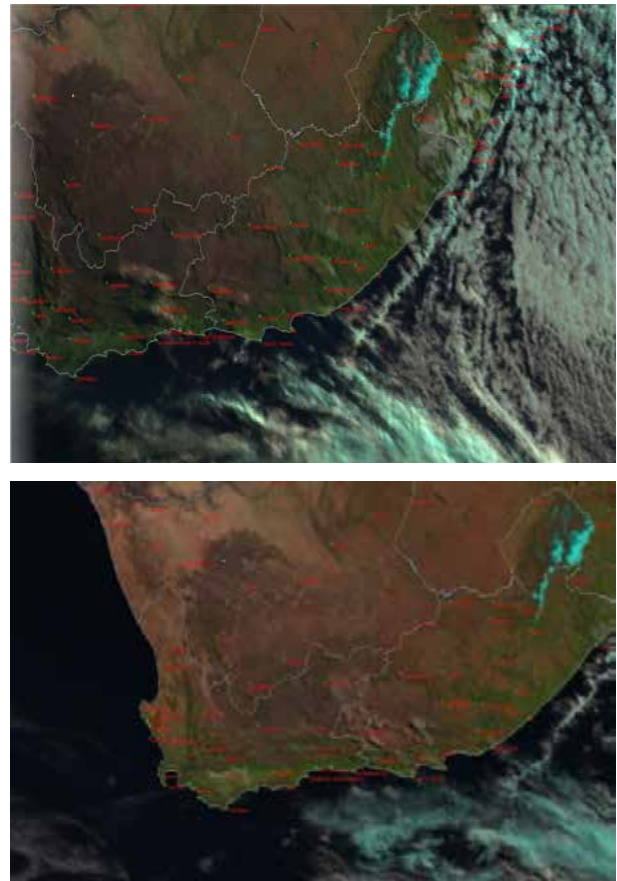


Figure 4: Satellite image showing snowfall over the southern Drakensberg on 4 June 2021 (EUMETSAT, 2021)

Daytime temperatures

These systems resulted in the first cold to very cold conditions of the winter season, with the daytime temperatures ranging between 5 to 10 °C over the north-eastern high ground from 1 to 3 June.

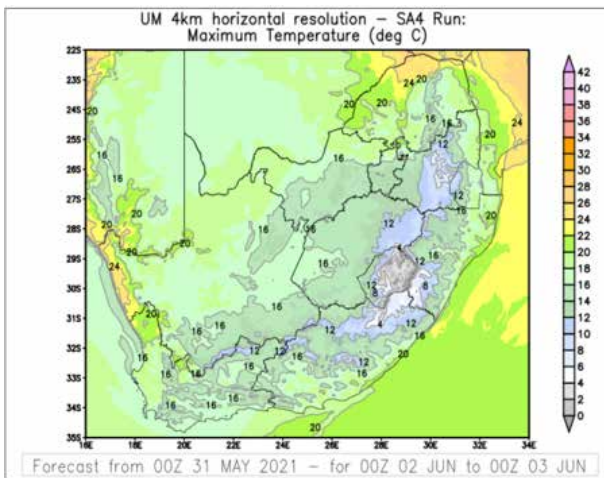
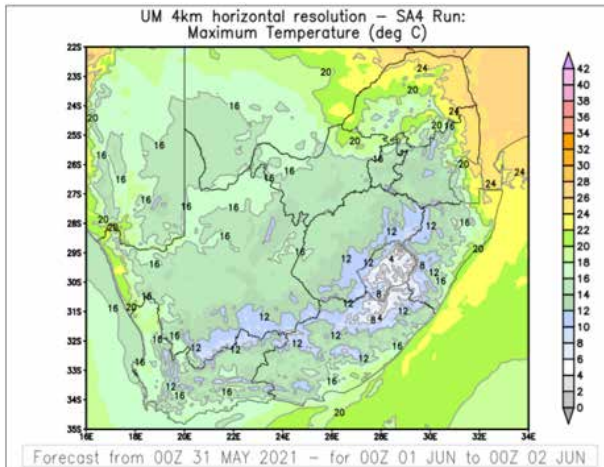


Figure 5: Expected daytime temperatures for 1 to 2 June 2021 over the Eastern Cape (UM SA4km)

Table 2: Observed daytime temperatures over the north-eastern highground.

Station	Temperature observations (°C)		
	01 June	02 June	03 June
Barkley East	07	09	09
Elliot	08	09	07
Molteno	10	09	09

Warnings Issued and observed impacts

Issued warnings

Figure 6 shows the warnings that were issued for the event, with the first warnings sent out on 31 May 2021, valid from 1 to 3 June 2021. Two snowfall warnings were issued, with a high likelihood of minor impacts (yellow level 2) and a medium likelihood of significant impacts (orange level 5). Moreover, three rainfall warnings were sent out, a yellow level 2 and an orange level 5. The orange level 5 was later upgraded to a high likelihood of significant impacts (orange level 6).

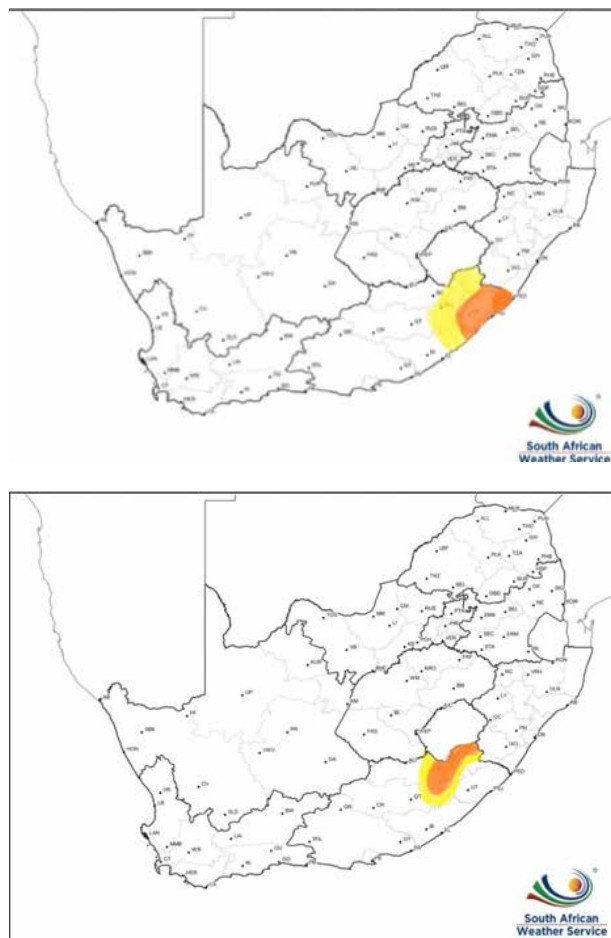


Figure 6: Issued IBF warnings for 1 to 3 June 2021

Table 3: Expected and observed rainfall impacts.

Rainfall	
Impacts expected	Impacts observed
Flooding (settlements)	 
Flooding (low-lying bridges/roads)	 
Communities cut-off/loss of livelihood	 
Rockfalls	 

Table 4: Table showing expected and observed snow impacts.

Snow	
Impacts expected	Impacts observed
Slippery roads	 
Traffic disruptions	 
Loss of livestock and crops	 
Accumulation of snow	 

Conclusion

The dominant systems which resulted in adverse weather conditions were captured well by the models, which then gave the forecasters confidence to issue snow and rainfall warnings ahead of time. Areas between Coffee Bay and Port Edward reported flooding of roads, settlements and low-lying bridges. Some communities were temporarily cut-off, with traffic disruptions observed due to flooded bridges.

Moreover, rockfalls and localised landslides were also observed. The accumulation of snow over the southern Drakensberg and surrounding areas resulted in slippery road conditions, traffic disruptions and loss of crops. Some incidents of livestock losses were also expected, although no reports were received.

Finally, an increased knowledge and skill in the different vulnerabilities and sensitivities of the various areas over the province will be of benefit in forecasting future impacts related to expected adverse weather.



The Performance Assessment of Six Global Horizontal Irradiance Clear Sky Models in Six Climatological Regions in South Africa

by Brighton Mabasa , Meena D. Lysko*, Henerica Tazvinga, Nosipho Zwane and Sabata J. Moloi*

1. Introduction

Clear sky models are used to estimate the amount of solar irradiance that reaches the Earth's surface under cloudless atmospheres. The global horizontal irradiation (GHI) clear sky radiation model is an algorithm that is solved by providing inputs that describe the state of the cloudiness atmosphere at a specific location and time to output theoretical GHI at that location and time [1]. In this study, the cloudless atmosphere is meant to exclude clouds but include aerosols. Clear sky irradiance data are important for various applications such as solar radiation forecasting and the calculation of maximum possible output yield of solar photovoltaic systems [1–9], cloudiness index calculation [2,3,5,7] and data quality control [3–7,10]. Clear sky solar irradiance is also used as the basis for deriving solar radiation estimates from satellite images [1,5,8,10], the calibration of sensors [3,4], the evaluation of cooling loads of commercial structures [1,4,5,8], the building of databases for testing radiation separation models [2,5], determining geographical areas where irradiance estimates are uncertain [4] and for the filling of missing historical data records [10].

There are no sensors to measure clear sky irradiance nor a universal model; the only way to generate clear sky irradiance data is by filtering in-situ readings taken from pyranometers for periods when there are no clouds or by trying different models at different locations. Various models have been developed, improved, and validated to estimate clear sky GHI data. Even though there are advanced methods to derive GHI data, ground monitoring using a pyranometer remains the most accurate way to collect data [11,12]. However, pyranometer measurements are limited or scarce due to the high costs involved in the installation, maintenance, and calibration of the sensors. The optical transparency of the atmosphere, physics of the model inputs and the effects thereof are still not fully understood [13], making it difficult to accurately model clear sky GHI.

The dynamic nature of the atmosphere results in biases when the modelled data are compared to data recorded using a reference pyranometer under clear skies.

The biases in different locations can only be quantified by the validation of models. Badescu et al., 2013 [10] emphasised the need for the validation of models because some models have never been validated in some regions with differences in atmospheric constituents to the areas where the models were developed. On the other hand, Antonanzas-Torres et al., 2019 [7] emphasised testing different models on a site because models perform differently. The validation of models is the best way to assess the suitability of different models in different areas other than where they were developed, for instance, in areas with different atmospheric content, albedo, latitude, and altitude.

According to Polo et al. [1], the major challenges in clear sky radiation model validation are the unavailability of high spatio-temporal atmospheric input parameters and not having access to specialised databases to be able to derive some of the atmospheric inputs that are not measured. The detection of clear sky days was also another challenge highlighted by [1]. In this study, to mitigate the challenges in the reviewed literature and to improve on what has been done, measured temperature, pressure and humidity from each of the stations have been used as inputs to the models. Meteorological input parameters which are not measured in-situ are attained from specialised databases. In this study, satellite albedo data are used instead of a suggested default value, such as 0.2 in Bird et al. [17,18].

The clearness index threshold (K_T), which is the ratio of $\frac{GHI}{GHI_{TOA}}$, is one of the methods that is used to classify clear sky times. From the studies, it has become evident that different areas or climates have different ratios. There is no standard scale and since K_T varies per site, the chosen ratio per site might not be accurate and might result in the classification of cloudy times as clear, introducing biases in the results.

* Non-SAWS

Clear sky times can be detected using observation cloud data or data from sky imagers. The challenge with this method is that observation cloud data are scarce or only available at certain times and places. Moreover, clear sky imagers are not available to some meteorological institutions because they are expensive. In the area of study, there were no observation cloud data, no clear sky imagers and no standard ratio K_T for areas of the study. Clear sky days are therefore detected by using total cloud cover data from the fifth generation European Centre for Medium-Range Weather Forecasts (ECMWF) atmospheric reanalysis of the global climate (ERA5) [19] reanalysis dataset. Based on the literature review, no study has previously used this dataset to detect cloudless days for clear sky model studies. ERA5 data allow for more clear sky days to be detected and used. An additional methodology by Reno and Hansen (2016) [20] has been applied to filter out not clear sky times and outliers introduced by factors other than clouds which are too small to be detected by quality control methodologies.

From the different clear sky model validation studies reviewed, different models performed differently in different climates and the performances of the models were found to be influenced by the input parameters. It was also found that measured input parameters produced better results compared to default inputs and that some specialised gridded reanalysis databases are good model inputs. In South Africa, a few studies have been performed by [21–23]. They all used 1-year reference GHI data to validate the models, and at most eight locations were used by Zhandire (2017) [21]. However, those locations did not cover all climatic regions of the country and only four clear sky models were validated. Patel and Rix (2019) [22] validated two clear sky models in Stellenbosch using only one clear sky day per season and used the default inputs and not the real measurements. Javu et al., 2019 [23] used only five clear sky days for five locations and highlighted that it was not enough to fully assess the performance of clear

sky models. The validation of clear sky models is ongoing worldwide, but limited work has been performed in South Africa where all climatic zones are considered to determine the most suitable and better performing model which can be used to estimate minute GHI under clear sky conditions. In this paper, the performances of six GHI clear sky models, namely: Bird (1981) [17,18], Simple Solis (2008) [24,25], McClear (2013) [15], Ineichen–Perez (2002) [26,27], Haurwitz (1945) [28,29] and Berger–Duffie (1979) [30], are investigated relative to in-situ data from 13 South African Weather Services (SAWS) reference stations and across the diverse macro-climates in South Africa. This validation study covers more stations and uses more clear sky days than previous studies and enables a fuller assessment of clear sky models. The models were chosen based on the availability of inputs, implementability with open source (Python, from Amsterdam in the Netherlands), and their presence in the literature to enable the comparison with other validation results.

2. Data and Methodology

2.1 Data

The study area was determined by considering the locations of the SAWS radiometric stations which measure the 1-min GHI data. The area of study is thirteen sites located in all six macro-climate regions in South Africa. These macro-climate regions and the location of the 13 sites in the study area are shown on the map in Figure 1 (in the previous study). GHI data were collected using secondary standard, CMP11, Kipp and Zonen pyranometers. Hourly average values of temperature, humidity and pressure from areas corresponding to GHI measures were also collected.

The various clear sky models require different input parameters. Some input parameters are common. All the input parameters required by the six different models are summarised in Table 1.

Table 1. Model and input parameters required.

Input/Model	Bird	Simple Solis	Ineichen-Perez	McClea	Haurwitz	Berger-Duffie
Zenith Angle	X	X	X	X	X	X
Albedo	X	-	-	X	-	-
AOD1240nm	X	X	-	-	-	-
AOD550nm	X	X	-	X	-	-
AOD380nm	X	-	-	-	-	-
AOD500nm	X	-	-	-	-	-
AOD700nm	-	X	-	-	-	-
Temperature	X	X	-	X	-	-
Humidity	X	X	-	X	-	-
DNI_{TOA}	X	X	X	X	-	X
D (Julian day)	X	X	X	X	X	X
1367 (solar constant)	X	X	X	X (1362)	-	-
Pressure	X	X	X	X	-	-
Altitude	X	X	X	X	X	X
Linke Turbidity	-	-	X	-	-	-
Ozone	X	-	-	X	-	-
Absolute airmass	-	-	X	-	-	-
Relative airmass	X	-	X	-	-	-
Apparent Elevation	-	X	-	-	-	-
Asymmetry	X	-	-	-	-	-
Total inputs	16	13	9	12	3	4

2.2 Methodology

The methodology used in this study is summarized in the flow chart in Figure 1 below. The methodology consists of eight steps as follows:

1. Detection of clear sky days using the ERA5 hourly reanalysis data set [19];
2. Preprocessing of observation data and BSRN quality check [55,56];
3. Identification of 1-min clear sky periods;
4. Configuration and running models on clear sky days;
5. Application of the additional clear sky periods detection method [20];

6. Matching common time steps of observation and modelled data;
7. Division of the common time steps into 5 degree zenithal angles; and
8. Calculation of statistical metrics for each 5 degree zenith bin.

The statistical metrics that were used to compare estimated 1-min clear sky GHI data with the observed 1-min GHI data were relative Mean Bias Error (*rMBE*), relative Root Mean Square Error (*rRMSE*) and Coefficient of Determination (R^2).

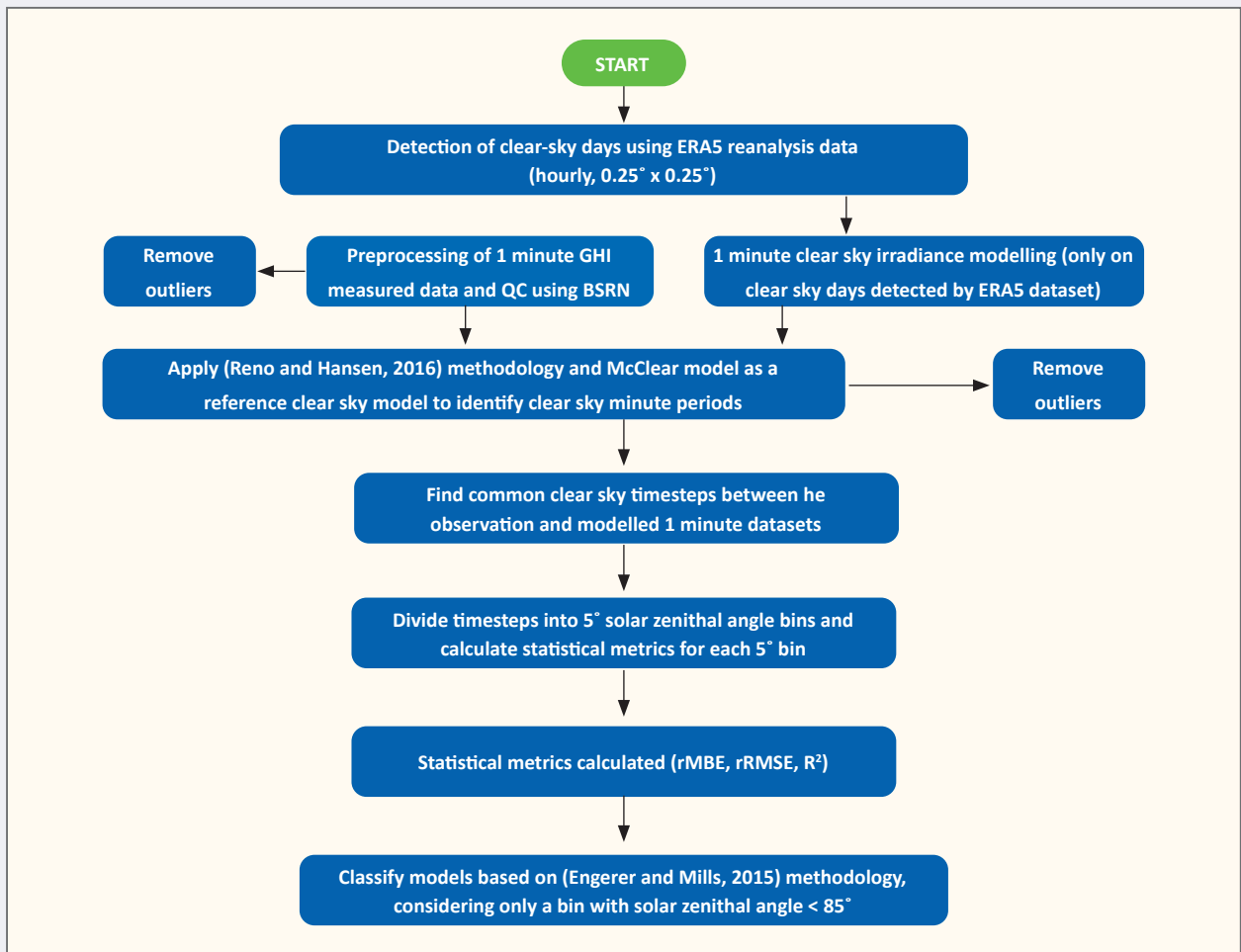


Figure 1. The flowchart of the approach summarising the methodology from clear sky detection to model classification based on their performance. {Fifth generation European Centre for Medium-Range Weather Forecasts atmospheric reanalysis (ERA5); Global horizontal irradiance (GHI); Quality control (QC); Baseline Surface Radiation Network (BSRN)}.

3. Results and Discussions

3.1. Clear Sky Detection

The ERA5 hourly reanalysis data set can also be used to detect cloud sky days—even though one of the clear sky model’s applications is to determine the upper bound of GHI, it is worth knowing that in some cases when there are clouds the measured instantaneous GHI can surpass the clear sky boundary but it cannot surpass the GHI_{TOA} . According to Dazhi et al., 2015 [7], the reason behind this is the reflection from the clouds, and according to Long and Shi (2008) [58], it is because of the enhancement of the DIF and then the DNI not being blocked by clouds for short periods.

An additional clear sky detection methodology, such as that by Reno and Hansen 2016 [20], is needed to remove outliers other than clouds. The Reno and Hansen method has been applied in this study to detect observation

errors that are not picked out automatically with the quality control procedures. Reno and Hansen 2016 [20] method successfully detected some errors missed by quality control procedures, the detected errors can be removed by the user.

3.2. Validation Results

After detecting clear sky times, a random set of days for each of the 13 stations is shown in Figures 2–4. All the models generated data that captured temporal variability but with varying accuracy. Additionally, a summary of performance is given in Tables 2 shows the optimum model w.r.t metrics for each station, whilst Table 3 shows the number of stations where a model shows an optimum metric. An optimum model per metric and station is found as follows: minimum $rMBE$, minimum $rRMSE$ and maximum R^2 .

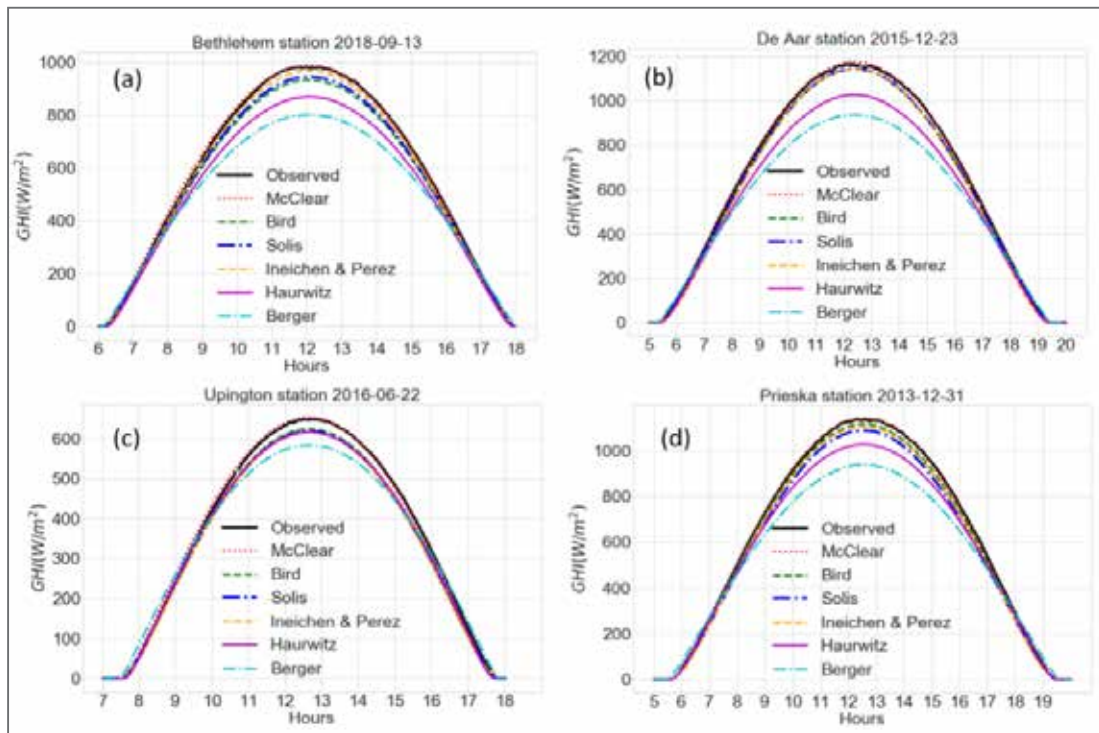


Figure 2. Comparison between observed and modelled minute GHI values in Bethlehem (a), De Aar (b), Upington (c), and Prieska (d).

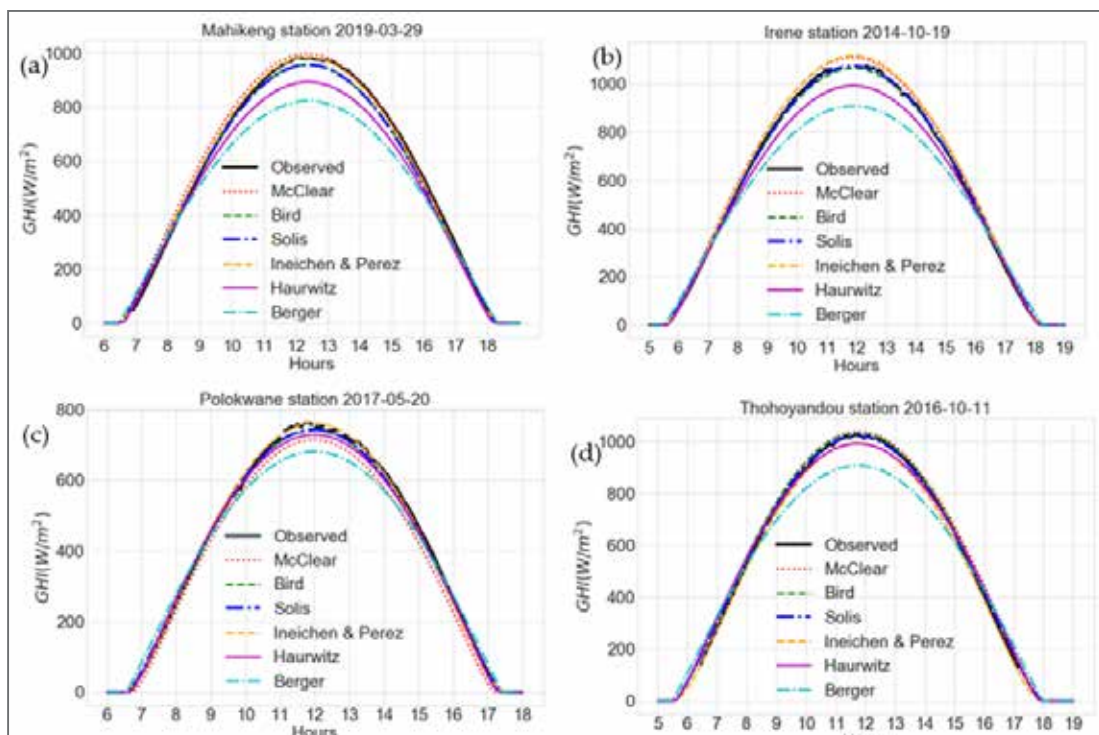


Figure 3. Comparison between observed and modelled minute GHI values in Mahikeng (a), Irene (b), Polokwane (c), and Thohoyandou (d).

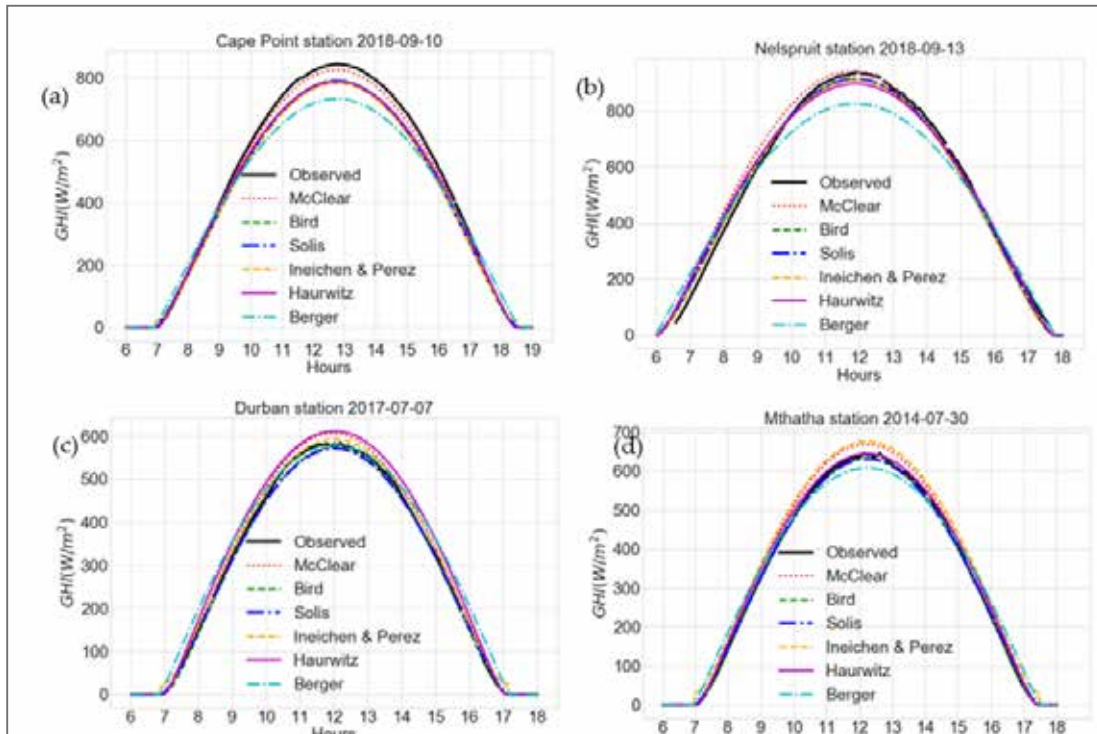


Figure 4. Comparison between observed and modelled minute GHI values in Cape Point (a), Nelspruit (b), Durban (c), and Mthatha (d).

Table 2. Optimum model w.r.t metrics for each station (colour codes indicate different climatic zones)

Station	Minimum $rMBE$	Minimum $rRMSE$	Maximum R^2
Cape Point	Berger-Duffie	McClea	McClea
George	McClea	McClea	Bird
De Aar	Simple Solis	Bird	Bird
Bethlehem	Simple Solis	Simple Solis	Bird
Uppington	McClea	McClea	McClea
Prieska	Bird	Bird	Bird
Mthatha	Haurwitz	Bird	Bird
Durban	Bird	Bird	Bird
Mahikeng	Ineichen-Perez	Ineichen-Perez	McClea
Irene	Simple Solis	Simple Solis	Bird
Polokwane	Simple Solis	Bird	Bird
Thohoyandou	Ineichen-Perez	Ineichen-Perez	McClea
Nelspruit	Simple Solis	Bird	Bird

From Table 2 and 3, Bird Model had a better performance that all the models with minimum $rRMSE$ in 6/13 (46%) and maximum r^2 in 9/13 (69%) stations. The better results might be because of using monthly satellite albedo instead of a default value, calculating P_w from measured temperature and humidity instead of climatologies, and using actual station pressure. O_3 was the only input that

was sourced as monthly climatology values from SoDa [38]. According to Bird et al (1981) [17], O_3 have a minor effect on irradiance and Polo et al. [1] reported that the variability of daily O_3 ozone is low.

McClea model was only outperformed by Bird in South African locations. This may mean that “black box”

model need further improvement to be able to estimate irradiance with better accuracy than Bird model in South African locations. Still, the McClear model performs good and it has an advantage over all other models because the data is readily available, no need to configure and provide input parameters.

Simple Solis was only outperformed by Bird and McClear models in South African locations. The better results might be because of using high spatiotemporal resolution model inputs, using actual station pressure, daily AOD_{700} from SoDa [38] and P_w calculated from measured temperature and humidity.

Table 3. Indication of number of stations with an optimum metric

	Number of stations with minimum $rMBE$	Number of stations with minimum $rRMSE$	Number of stations with maximum R^2
Berger-Duffie	1	0	0
Bird	2	6	9
McCclear	2	3	4
Haurwitz	1	0	0
Ineichen-Perez	2	2	0
Simple Solis	5	2	0

Ineichen–Perez clear sky model performed less fairly, when compared against other complex models. This might be because Ineichen–Perez is the only model that depends on TL as an input. The TL data was sourced as monthly climatologies from SoDa [38]. According to Ineichen (2006) [16], TL has the highest influence on model accuracy. The model accuracy might improve with locally measured TL, though TL observations were not available in the area of study.

Haurwitz clear sky model performed had a performance, the poor performance of the model may be a result of the calibration of the Haurwitz model. The Blue Hill observatory where the coefficients a and b were calibrated have different atmospheric constituents to South African locations. There is a need to calibrate coefficients a and b using data measured from South African locations.

Berger-Duffie clear sky model had a poor performance in all the locations. It underestimated irradiance in

almost all the South African sites except in Durban. The poor performance shows that the transmittance of the model, which was integrated to a constant of 0.7 need to be recalibrated for each of the South African sites to be able to estimate GHI under clear sky accurately.

4. Conclusions

In this study, the performance of six GHI clear sky models, namely Bird, Simple Solis, McClear, Ineichen–Perez, Haurwitz and Berger–Duffie, have been evaluated against reference Baseline Solar Radiation Network quality guided 1-min data for 13 stations in the South African Weather Services radiometric network. The stations are located in six climatological regions. All the models assessed were capable of reproducing GHI irradiance, but with different accuracy in different stations. All four complex models, namely Bird, Simple Solis, McClear and Ineichen–Perez, performed well with $rRMSE$ less than 10% in all the stations. The simple models, Haurwitz and Berger–Duffie, did not perform well overall in South African locations. Bird was the overall best model, followed by Simple Solis, McClear, Ineichen–Perez, Haurwitz and Berger–Duffie. The McClear model overestimated GHI and the other five models underestimated GHI. Model inputs seem to influence the model performance. There is also an indication that each model behaves differently over particular climate regions.

Future studies will focus on validating more clear sky GHI models and other solar radiation parameters and optimising or calibrating simple models’ coefficients for each site. Future work will also focus on sourcing high temporal and spatial resolution model inputs from different databases and trying to re-validate models to find suitable model inputs. Future studies will also focus on using the results for renewable energy applications.

The challenge encountered in the study was the absence of high temporal and spatial resolution model inputs. It is recommended that GHI monitoring stations also measure high temporal and high spatial resolution water vapour, aerosols, ozone and albedo to aid model assessment studies.

<https://www.mdpi.com/1996-1073/14/9/2583>

The Ångström–Prescott Regression Coefficients for Six Climatic Zones in South Africa

by Brighton Mabasa, Meena D. Lysko*, Henerica Tazvinga, Sophie T. Mulaudzi, Nosipho Zwane and Sabata J. Moloï*

1. Introduction

Solar radiation data are important because they are required in many research fields such as meteorology, agriculture, hydrology, ecology, and environment [1–4]. Solar radiation data are also an important reference for many applications such as solar power plants, engineering designs, regional crop growth modelling, evapotranspiration estimation, and irrigation system development [1,3,5]. In relation to this, South African Weather Services (SAWS) re-established a global horizontal irradiance (*GHI*) radiometric network with 13 solar radiometric stations located in all 6 macroclimatic zones of South Africa [6]. The macroclimatic zones are regions with similar climatic conditions, and they were established to classify different areas based on their maximum energy demand and maximum energy consumption [6]. The data collected from the SAWS network help in the validation of satellites as well as the development and verification of empirical models [7]. SAWS also manage a very dense sunshine duration recording network over South Africa to the extent that sunshine duration data have been continuously measured for several years [8]. SAWS *GHI* stations are sparse; according to [1–5,9], having dense radiometric networks is a worldwide challenge because of the high costs involved in the installation and maintenance of the solar radiation stations. To compensate for this, reliable measurements taken from a sparse network are needed to develop and validate empirical models that can be used to estimate and forecast the availability of solar energy at other locations [10]. The main objective of this study is to calibrate the Ångström–Prescott (AP) model regression coefficients a and b that could be used to estimate *GHI* in different climatic zones of South Africa, thus increasing the density of available solar radiation data in the country.

The AP model estimates daily *GHI* using daily top of the atmosphere *GHI* radiation (GHI_{TOA}), daily astronomical day length (N), daily measured sunshine duration (n), and Ångström model coefficients a and b . The model was first proposed by Ångström [11] in 1924 before Prescott [12] modified it in 1940 by adding GHI_{TOA} to replace *GHI* on a clear sky day. The original AP coefficients were $a =$

0.25 and $b = 0.75$; these were calculated using data from Stockholm [13]. The regression coefficients a and b are site-dependent; therefore, there is a need to calibrate them using a linear relationship in Equation (1) at regions where they will be used to estimate *GHI* [1,4,13,14].

In South Africa, studies to calibrate AP coefficients were carried out by Eberhard [17] and Mulaudzi et al. [18]. The challenge, according to Mulaudzi et al. [18], was the unavailability of a long-term observation *GHI* dataset that covers all the climatic regions to calibrate and validate the AP coefficients. In this study, a large enough dataset with observations spanning 2013 to 2019 from stations that cover all the climatological zones of South Africa was used to calibrate the AP coefficients, which were then used to estimate *GHI*. The estimated *GHI* was validated using the observed *GHI* daily averages, while the statistical metrics were used to quantify the differences between observed and estimated *GHI*.

From the results of this study, annual AP coefficients a and b in all six macro-climatological regions could be used to estimate daily *GHI*, for the respective climate regions, using daily observation sunshine duration data. The knowledge of estimated daily *GHI* data can thereby be used to develop energy policies and solar energy programmes. They can also be used as benchmarks in climate analysis studies.

2. Materials and Methods

The observed 1-min *GHI* data used in this study were collected from 8 SAWS solar radiometric stations during the periods shown in Figure 1, which also shows the climatic zones in which the stations are located. *GHI* data were collected using secondary standard, CMP11, Kipp and Zonen pyranometers.

The methodology is provided in the flowchart in Figures 2. Daily *GHI* data were calculated from 1-min *GHI* data. First, the 1-min *GHI* data were quality controlled using a Baseline Solar Radiation Network (BSRN) quality control (QC) procedure outlined by Long and Dutton in [21]. Minute values that passed the BSRN QC were averaged to 15 min and then, 4 slots of 15-min averages were averaged to obtain an hourly mean [6,7,22–25].

* Non-SAWS

Hourly mean values were then averaged to obtain daily average values. Daily average values were further quality checked by subjecting them to HelioClim model QC, described by Geiger et al. in [26].

Hourly sunshine duration data were obtained by determining the burn made by the sun on a coated card in a Campbell–Stokes sunshine recorder [8]. Hourly data were then summed to obtain total daily sunshine duration (n). Daily top-of-atmosphere (TOA) irradiance (GHI_{TOA}) and theoretical sunshine duration (N) were calculated using Equations from Iqbal [13], and the solar angles were calculated using the Solar Position Algorithm (SPA) on Python PVLIB [27,28].

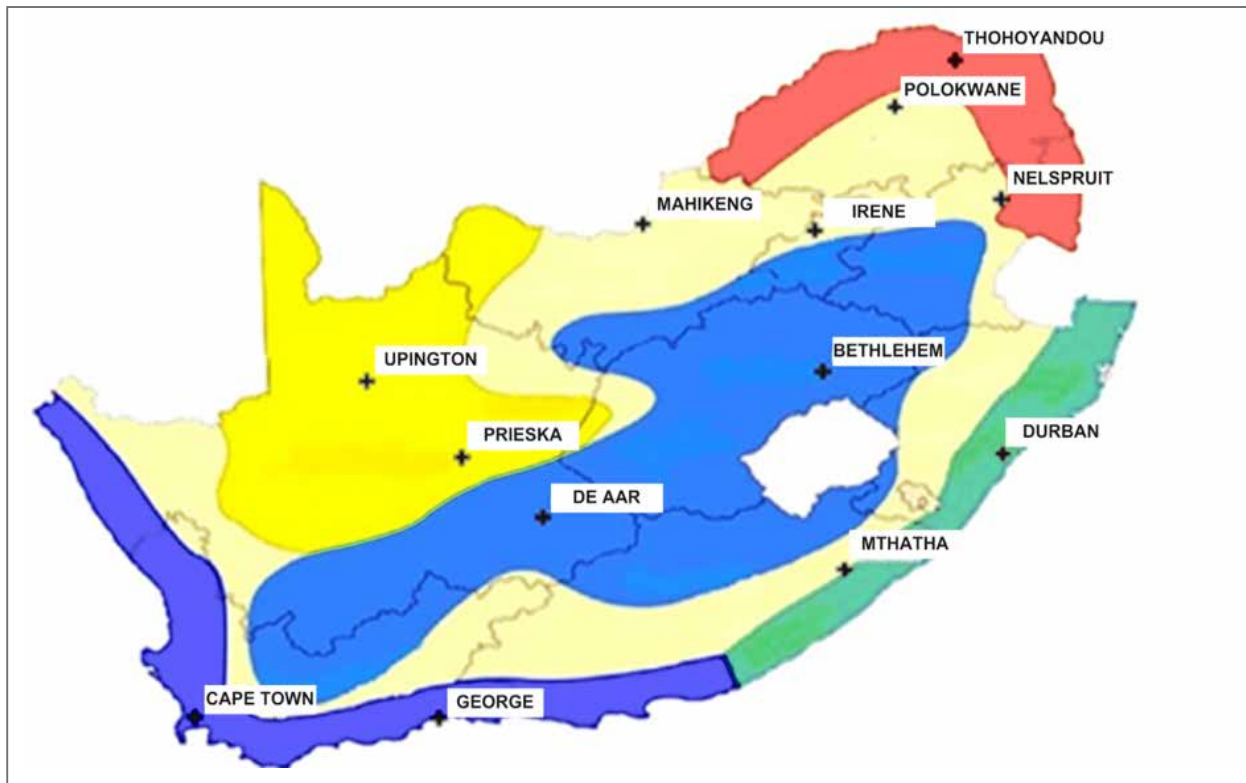


Figure 1. A map showing SAWS radiometric station location and climatic zones.

The coefficients a and b of the AP model were calculated by using the linear regression analysis between the irradiance fraction or clearness index, $\frac{GHI}{GHI_{TOA}}$ and daily sunshine fraction, $\frac{n}{N}$ for each day, based on a linear relationship shown by Equation (1) proposed by Ångström [11] and then, modified by Prescott [12].

$$\frac{GHI}{GHI_{TOA}} = a + b(n/N), \quad (1)$$

Annual AP coefficients were calculated for 8 stations. Datasets up to the end of 2018 were used for determination of the AP coefficients, and the daily observation data for 2019 were used to validate the corresponding estimated daily GHI data.

The statistical metrics Mean Bias Error (MBE), relative Mean Bias Error ($rMBE$), Mean Absolute Error (MAE), relative Mean Absolute Error ($rMAE$) and Coefficient of Determination (R^2) were used to compare estimated daily GHI data with the observed daily GHI data.

The results were converted from W/m^2 to $MJ\ m^{-2}d^{-1}$ by dividing by 11.57415, a methodology used by Almorox et al. [5] to allow for easy comparison with other literature studies. Monthly averages of each metric were calculated and then aggregated to annual averages, and where observation data were not available, data were replaced by NaN.

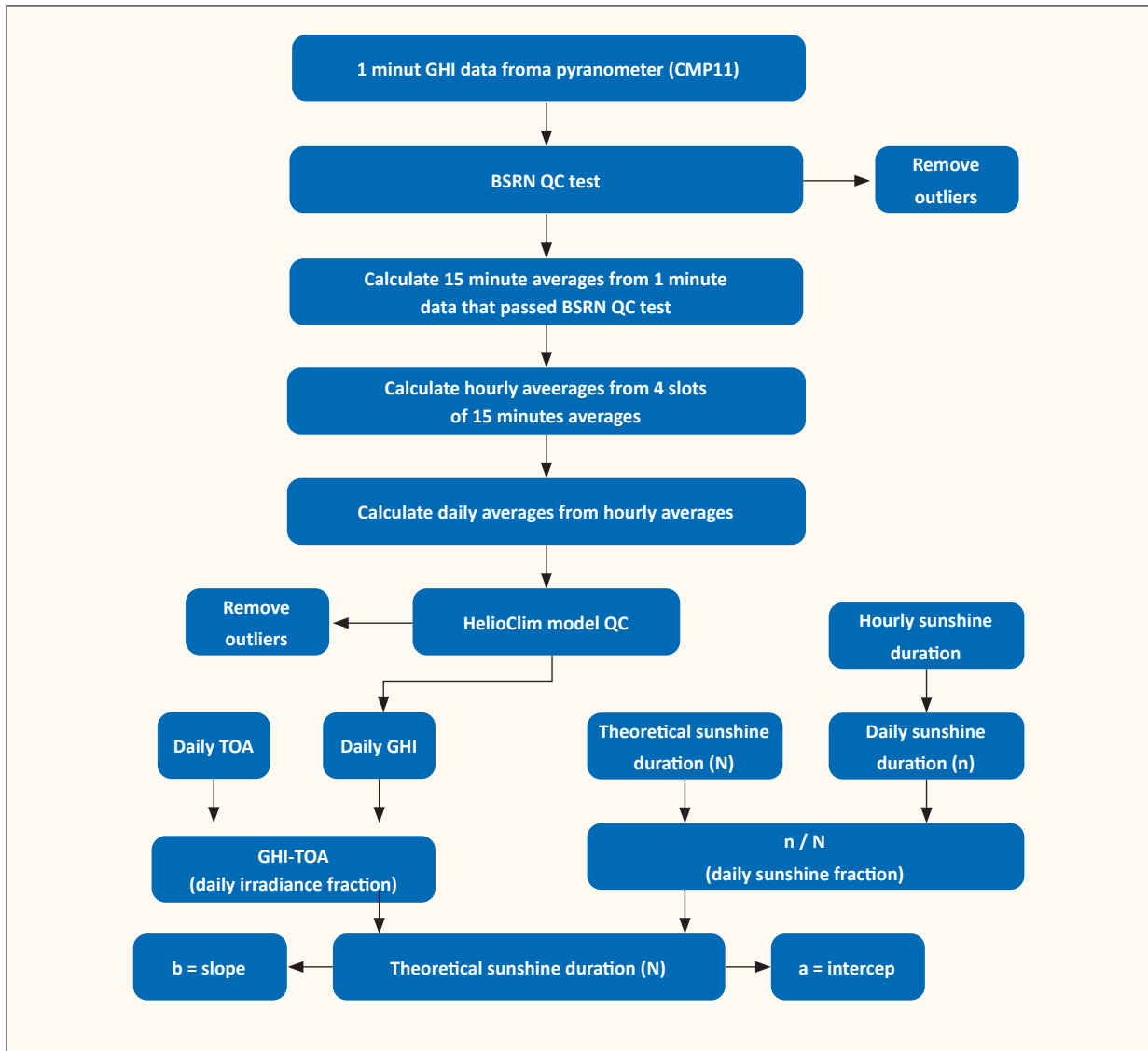


Figure 2. The flowchart of the approach used to calculate Ångström–Prescott regression coefficients a and b .

3. Results and Discussion

3.1. Annual AP Results

In this study, the annual AP regression coefficients a and b were calculated using Equation (1) and the following variables daily n , daily mean GHI , daily mean GHI_{TOA} , and daily N were used as inputs. The calculated a and b were then used together with daily n and N to estimate daily GHI , which was then compared to corresponding observed daily GHI . Statistical metrics were used to quantify the errors between the two datasets; the results are shown in Table 1 and Figures 3–6.

In Figures 3 and 4, the annual AP coefficients and the data points that were used to derive them are displayed. The values of the AP coefficients ranged from 0.188 to 0.243 for a , while those for b ranged from 0.515 to 0.6. Values of $a = 0.25$ and $b = 0.5$ were recommended by Allen et al. [31] to be used when there is no local observation GHI data to calibrate the coefficients. The minimum value of a in this study was less than 0.25 and the maximum value was greater than 0.25; the minimum and maximum values of b were greater than 0.5. The difference in default AP coefficients and calibrated AP coefficients proved that calibrating the coefficients locally is a necessity.

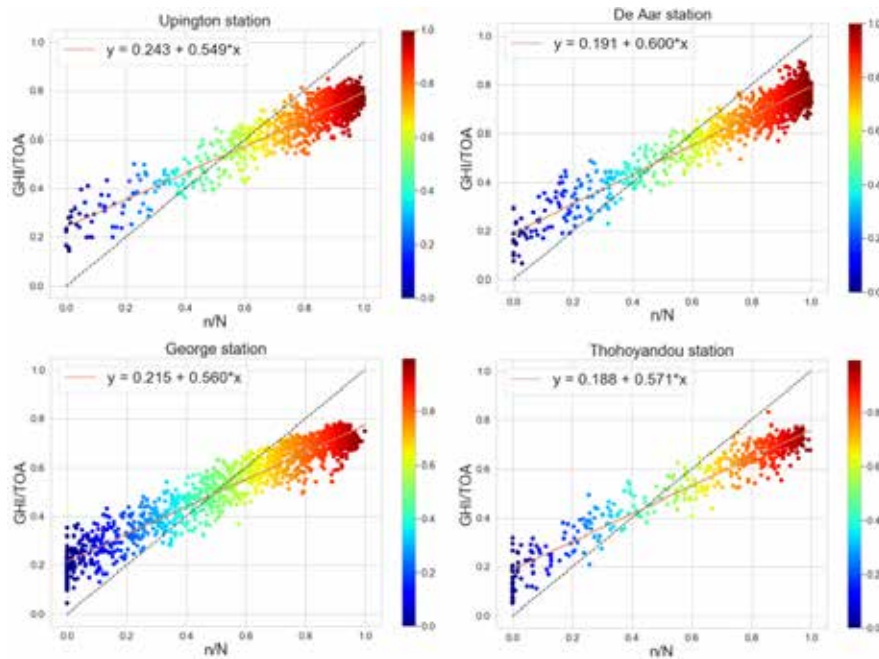


Figure 3. Regression lines and AP (the Ångström–Prescott) coefficients for Uppington station (top left), De Aar (top right), George (bottom left), and Thohoyandou (bottom right).

Studies done by Zhang et al., De Medeiros et al., Almorox et al., and Tsung et al. in [3–5,14] also found different results to Allen et al. [31] when they did a local calibration. When comparing the factors for stations that are located in the same climatological zone such as Irene and Polokwane located in the Temperature Interior climatic zone, and Mthatha and Durban in the Tropical Coastal climatic zone, the difference was less than 0.05 for both a and b , which is a very small difference. This means that the AP coefficients a and b calibrated for a climatic zone could be used as a representative for an entire climatic zone to estimate GHI when observed sunshine duration data for the location are available.

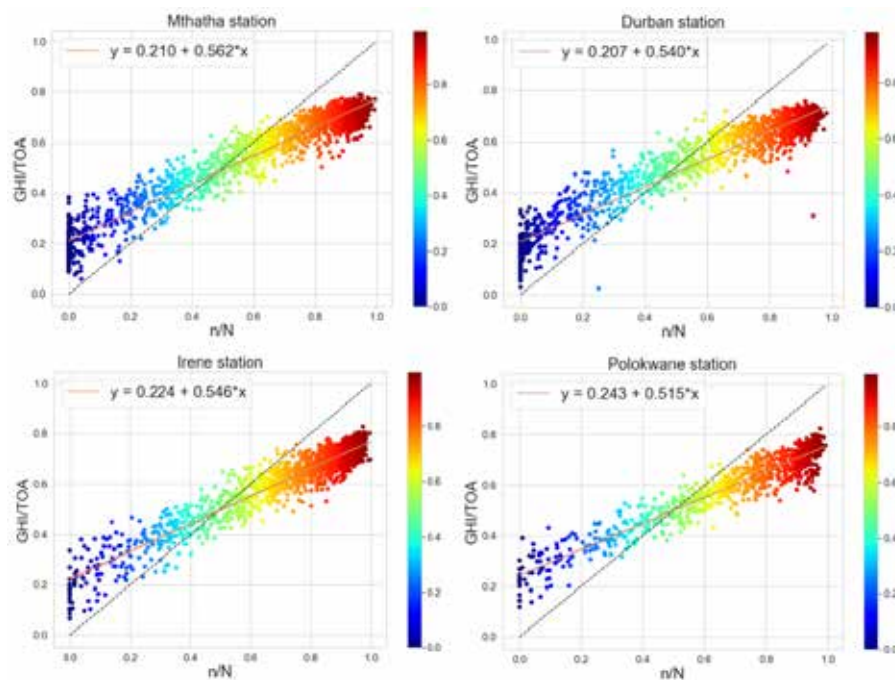


Figure 4. Regression lines and AP coefficients for Mthatha station (top left), Durban station (top right), Irene station (bottom left), and Polokwane (bottom right).

3.2. Validation Results

Estimated *GHI* values were compared to the measured *GHI* values; errors were quantified by validation metrics and the results were tabulated in Table 1. In Table 1, the *rMBE* ranged from -1.20 to 0.371%, *rMAE* from 0.311 to 0.745%, *rRMSE* from 0.393 to 0.910%, and R^2 from 0.910 to 0.948. De Aar, Irene, and Thohoyandou had a positive *MBE*, meaning that the model overestimated *GHI*, while Upington, Durban, Mthatha, George, and Polokwane had a negative *MBE*, meaning that the model underestimated *GHI* values at these locations. The values of *MBE* and *rMBE* for all the stations were less than 1, indicating that there was a strong correlation between the predicted and observed *GHI* values. The worst case R^2 value was 0.910, suggesting that there is a very strong linear relation between observed and predicted values.

The maximum *RMSE* of 1.741 MJ m⁻²d⁻¹ was less than 1.94 and 1.9 MJ m⁻²d⁻¹ that De Medeiros et al. [4] and Tsung et al. [14], respectively, determined. The maximum *MAE* of 1.425 MJ m⁻²d⁻¹ was less than 1.8 MJ m⁻²d⁻¹ that Tsung et al. [14] determined. The maximum *MBE* of 0.733 MJ m⁻²d⁻¹ was less than 1.040 and 0.85 MJ m⁻²d⁻¹ that De Medeiros et al. [4] and Tsung et al. [14], respectively, determined, and the worst case R^2 of 0.910 was greater than 0.875, 0.74, and 0.58 that Zhang et al. [3], Adamala et al. [2], and De Medeiros et al. [4], respectively, determined. As shown in Table 2, the results across the range of climate zones (including the ones from the literature), all differ significantly.

Table 2. Calibration coefficients *a* and *b* and validation metrics results in (MJ m⁻²d⁻¹).

Station	<i>a</i>	<i>b</i>	<i>RMBE</i>	<i>rMBE</i> (%)	<i>MAE</i>	<i>rMAE</i> (%)	<i>RMSE</i>	<i>rRMSE</i> (%)	R^2
Upington	0.243	0.549	-0.360	-0.120	0.841	0.311	1.061	0.393	0.930
De Aar	0.191	0.600	0.733	0.371	1.136	0.506	1.375	0.598	0.930
Irene	0.224	0.546	0.689	0.353	1.328	0.608	1.618	0.729	0.912
Mthatha	0.210	0.562	-0.104	-0.013	1.168	0.582	1.474	0.735	0.951
George	0.215	0.560	-0.270	-0.036	1.261	0.636	1.520	0.769	0.948
Durban	0.207	0.540	-0.322	-0.106	1.425	0.745	1.741	0.910	0.915
Polokwane	0.243	0.515	-0.286	-0.085	1.272	0.488	1.572	0.606	0.910
Thohoyandou	0.188	0.571	0.286	0.168	1.071	0.550	1.433	0.746	0.937
Almorox et al.	0.287	0.452	-0.002	-	-	-	1.260	-	-
De Medeiros et al.	0.39	0.29	1.040	6.29	-	-	1.94	-	0.58
Tsung et al.	0.5	0.11	0.85	3.4	1.8	-	1.9	-	-
Zhang et al.	0.214	0.552	-	-	2.249	-	0.214	-	0.875
Adamala et al.	0.28	0.52	-	-	-	-	7.04	-	0.74

The overall validation results from this study are comparable and even better than what was found in similar studies like [2–5,15], which concluded that the AP coefficients could be used to estimate *GHI* with confidence based on those validation results. The data used in the study were collected using secondary standard pyranometers (CMP11), which, according to Urraca et al. [23], generate high quality records of *GHI*. Urraca et al. [23] found large and unstable validation errors from stations that uses second class pyranometers

and silicon-based photodiodes compared to the ones using CMP11. This might be because CMP11 gives an integrated measurement of the total *GHI* available under all conditions due to its capability to measure the total solar spectrum from 0.3 to 3 micrometres wavelength. CMP11 pyranometers' use very high-quality quartz double domes, which improve the stability of a calibration factor over time; it also improves directional response and reduces thermal offsets. The CMP11 can give correct integrated values over a day, with the use

of smaller sampling intervals. At SAWS, a sampling interval of 5 s is used and this enables sudden changes such as passing small clouds, birds sitting on top of the pyranometers, and some other factors that result in shading of pyranometers to be identified and factored in the data. It is noted that smaller sampling intervals are not possible with CMP11 predecessors. The CMP11 has a specified expected daily uncertainty of less than 2% [32,33].

GHI data were subjected to robust quality control methodologies BSRN QC [21] and HelioClim model QC [26] before any analysis and outliers which might affect the results were discarded. The use of Python codes in data analysis enabled big data to be handled much more efficiently and execution of a code in data analysis resulted in correct and consistent outputs; these are

some of the reasons why the results in this study are better. This means that the AP coefficients results from this study could also be used with confidence to estimate *GHI* in different climatological zones of South Africa.

In Figure 5, 2019 monthly *GHI* observed data were compared to corresponding estimated 2019 monthly *GHI* data. Thohoyandou is the only station where validation was done using 2017 monthly datasets and the observation data were only available from February to October (January, November, and December 2017 datasets were not available). The need to fill in missing data further motivates this study, i.e., development and validation of models, and the results of this study can be used to fill any missing monthly mean *GHI* values for South African locations.

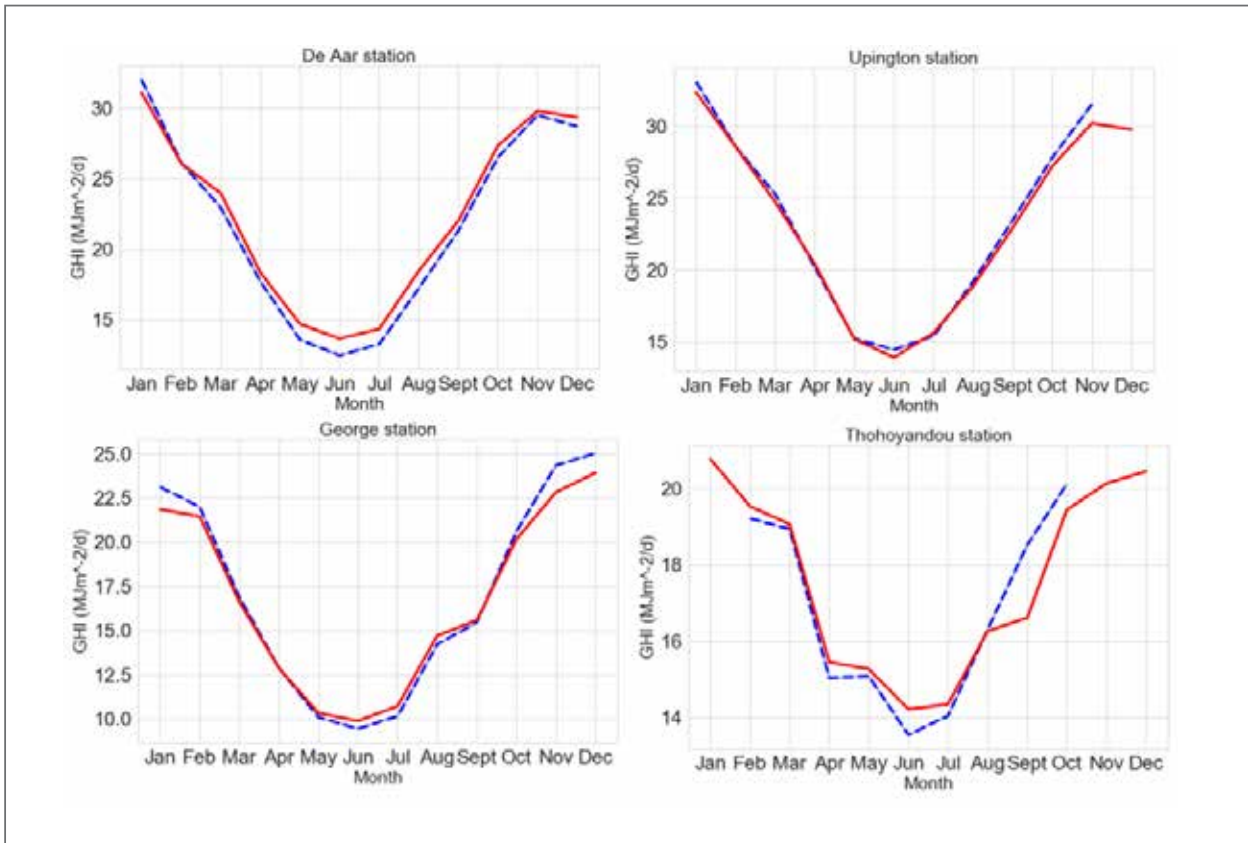


Figure 5. Comparison between measured and predicted monthly *GHI* values in De Aar (top left), Upington (top right), George (bottom left), and Thohoyandou (bottom right). Blue dotted line represents observed, *GHI* red solid line represents estimated *GHI*.

Similarly, in Figure 6, the 2019 monthly *GHI* observed data were compared to corresponding estimated 2019 monthly *GHI* data. In Durban, *GHI* observation data for September were not available. In Polokwane, the *GHI* observation data for March, April, May, and June were not available. The results from the study can be used to fill those missing monthly mean *GHI* values.

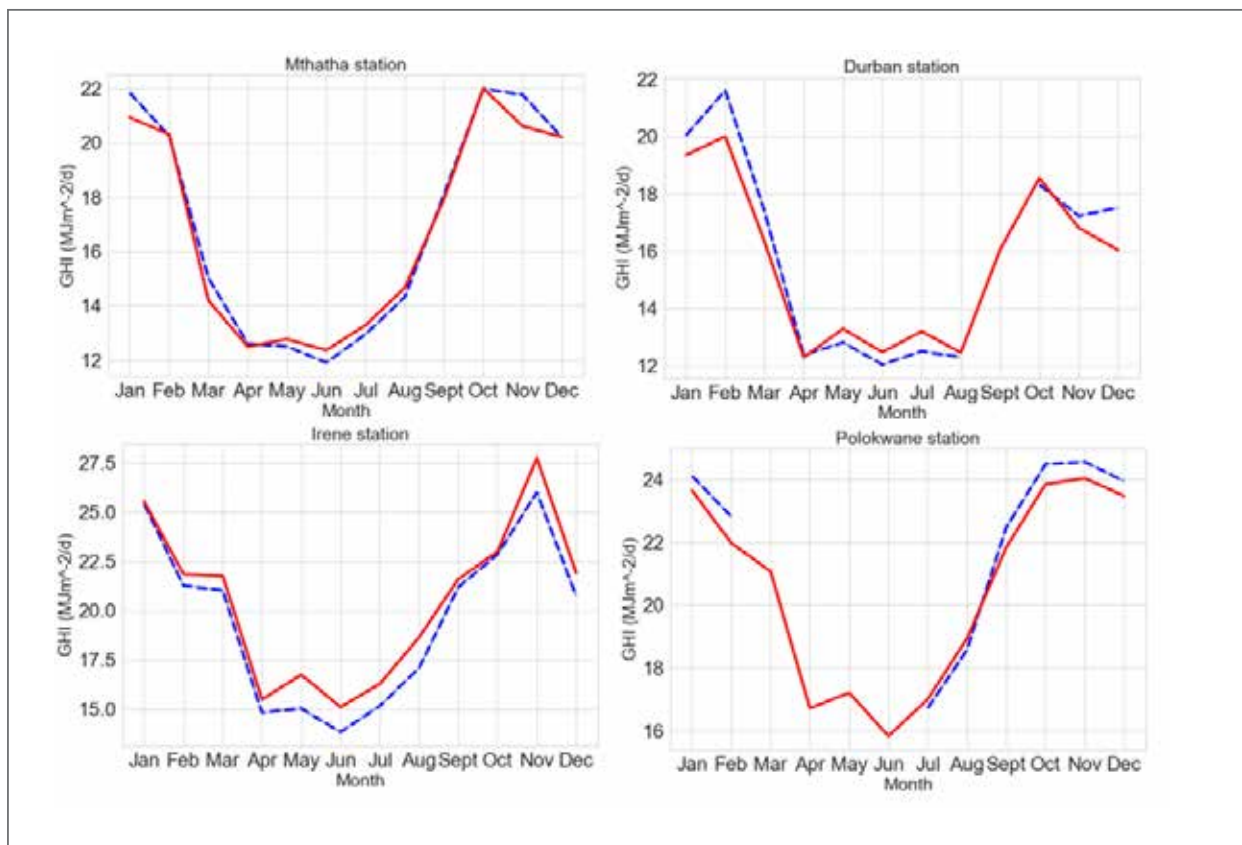


Figure 6. Comparison between measured and predicted *GHI* values in Mthatha (top left), Durban (top right), Irene (bottom left), and Polokwane (bottom right). Blue dotted line represents observed, red solid line represents estimated *GHI*.

4. Conclusions

The annual Ångström–Prescott coefficients a and b were calculated using the linear relationship between ratio of daily global radiation on a horizontal surface to the daily projected extra-terrestrial radiation on that surface and the ratio of daily sunshine duration to the theoretical sunshine duration. They were used to estimate global horizontal irradiance and there was a very close agreement with the corresponding observation global horizontal irradiance. The agreement was quantified by statistical metrics.

The methodology used in the study can be applied elsewhere, where there is a station that records global horizontal irradiance and sunshine duration. Practitioners need to cross check against their climate zones and not use a and b from one site to represent the entire country, as it varies per climatic zone due to variations in latitude, cloud cover, aerosols, surface albedo, and day lengths. The unavailability of confident observation of daily sunshine data in some areas might be a drawback for other practitioners.

Further research will focus on extended monitoring of the stability of the coefficients over time in each climate zone. Further research will also focus on calibrating and validating rainfall, cloud, temperature, and humidity-based models in areas where sunshine data are not recorded to make sure that daily global solar radiation data can be estimated in those areas in South Africa.

The Ångström–Prescott coefficients calibrated for each station can be used as a representative for the climatic zone where that station is located. The Ångström–Prescott coefficients calculated in this study could enable the estimation of daily global horizontal irradiance data at any location in South Africa, where daily observation sunshine duration data are available, and the climate is correctly classified. The knowledge of estimated daily global horizontal irradiance data can thereby be used to support energy policies and solar energy programmes. They can also be used as benchmarking in climate analysis studies.

<https://www.mdpi.com/1996-1073/13/20/5418>

Devastating fires on Table Mountain at the University of Cape Town: 18 to 20 April 2021

by Ntshalle Stella Nake, Cape Town Weather Office



Overview

Wildfires are a common feature in the City of Cape Town (CoCT) Municipality and the Western Cape province at large due to the native fynbos vegetation which is prone to fires. While many wildfires cause minimal damage to the land and pose few threats to the people in the neighbourhoods, some fires cause extensive damage that require special response efforts to prevent problems afterwards. An episode of these wildfires occurred on the slopes of Table Mountain on Sunday morning, 18 April 2021 around 08:45 (SAST). The fires affected a wide area compared to the previous fire incident that occurred on the mountain. The fire continued throughout Sunday and was contained only at 13:30 SAST on Tuesday, 20 April 2021. There were no fatalities reported but some notable fire damage included severe damage to the Rhodes Memorial restaurant, a historic windmill and the upper campus of University of Cape Town.

Historically, wildfires have been described as having two forces of ignition: environmental (which are beyond our control) and human-related (which are controllable). Many wildfires start from natural causes such as high atmospheric temperatures and dryness (low humidity) and to a lesser extent, lightning from a thunderstorm. Additionally, the environmental causes are largely related to climatic conditions such as temperature, wind speed and direction, the level of moisture in the soil and atmosphere, and duration of dry spells. Human-related causes can be either intentional, such as arson, or unintentional, for example controlled burns for land clearing and agriculture, and for removing dead trees or drying trees.

Synoptic Influence

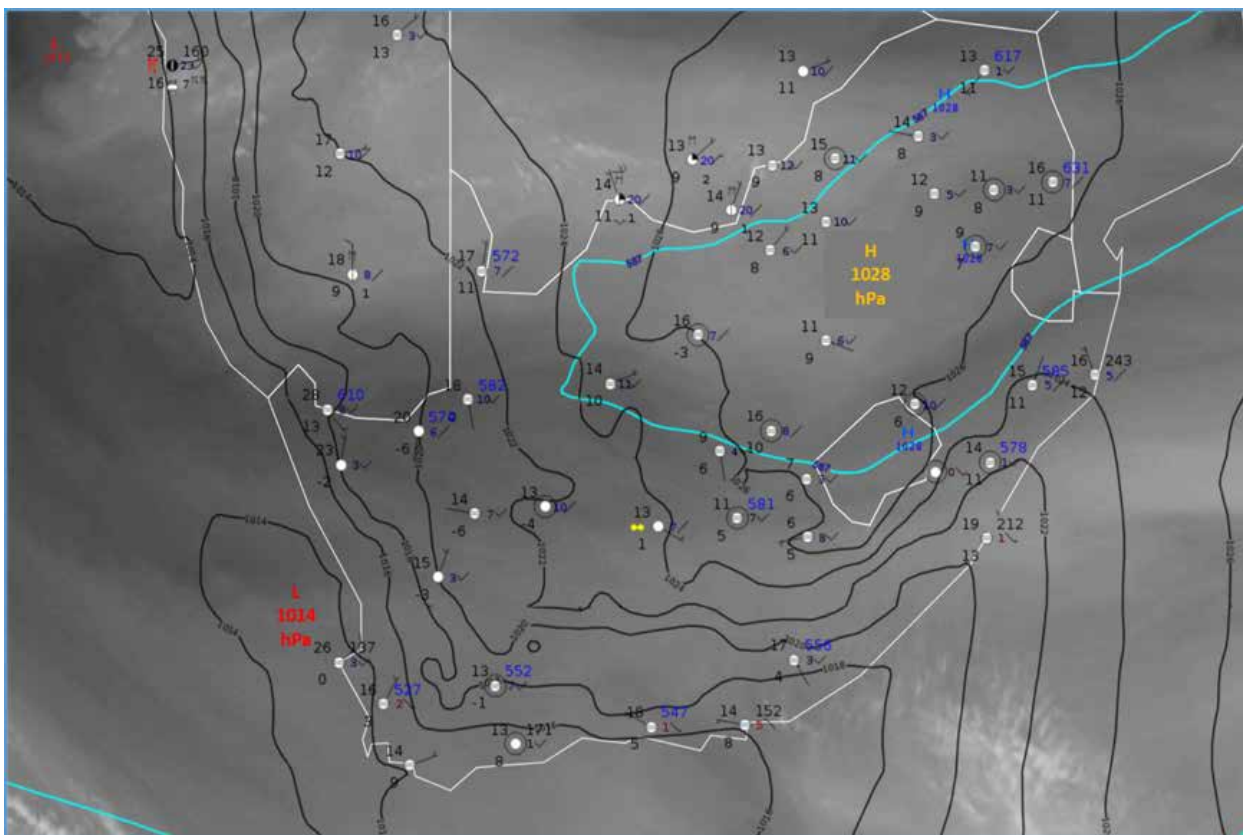


Figure 1: Water Vapour Satellite image overlaid with 500hPa geopotential heights (magenta lines), mean sea level pressure (black lines) & surface observations 2am, 18 April 2021 (Courtesy, EUMETSAT)

An upper-air high pressure system was situated over the north-eastern interior of South Africa. At the surface, an area of low pressure was situated along the south-west coastline with high pressure over the north-eastern interior (Figure 1). The typical weather conditions associated with the positioning of these weather systems over the western interior are mostly clear skies and warm to hot temperatures. Winds are usually light, becoming gusty in the late morning hours, peaking in the afternoon due to surface heating. The result of this gustiness is that the direction and speed of the wind at the higher levels (e.g., 4000 feet) tend to be transferred to the surface; and as the air descends, it warms dry adiabatically resulting in bergwind conditions over coastal areas.

On Sunday morning, dry conditions with light east to north-easterly winds (Figure 1) prevailed across most parts of the country, particularly the Western Cape. Due to dry and warm to hot conditions expected during the day, the South African Weather Service issued two weather warnings; firstly, a heatwave advisory for the West Coast District Municipality in the Western Cape, as well as a fire danger warning for most parts of the Western Cape. These weather conditions were expected to persist throughout Sunday into the evening, with cooler north-westerly air moving in overnight from the Atlantic Ocean behind the coastal low pressure system.

Fire danger and weather forecasts

The South African Weather Service through its Weather Forecasting Offices, every day, forecasts a Fire Danger Index (FDI) which is based on the “Lowveld Fire Danger Rating System”, commonly in use in South Africa at this time. The FDIs are classified into five colour coded categories (Figure 2), and when calculations flag a RED category (>75), a warning is published. This is in line with Chapter 3 of the National Veld and Forest Fire Act 1998, Act No 101 of 1998 on Fire Danger Rating.

Variables which are used to determine the FDIs are:

- Maximum Temperature
- Minimum Relative Humidity
- Highest hourly averaged wind speed
- Last 21 days of rainfall, which gives an indication of fuel dryness

High temperature combined with low relative humidity will lead to a high risk of ignition of wildfires. The risk of these fires developing to “runaway” (uncontrollable) fires increases as the wind speed increases and the fuel becomes drier.

On 18 April 2021, the FDI values across the weather stations in the City of Cape Town, did not meet the warning threshold (>75) and as a result, there was no fire danger warning issued for the City. However, there are other detailed 3-day fire weather products that get disseminated on a daily basis by SAWS to the fire management authorities, which help with their fire planning.

Lowveld FDI Description	Colour	Category	Lowveld FDI Precaution
SAFE	BLU	0-20	Low fire hazard. Controlled bum operations can normally be executed with a reasonable degree of safety
MODERATE	GREEN	21-45	Although controlled burning operations can be executed without creating a fire hazard. Care must be taken when burning on exposed, dry slopes. Keep constant watch for unexpected wind speed and direction changes
DANGEROUS	YELLOW	46-60	Controlled b1u11ing not recommended when fire danger index exceeds 45. Aircraft should be called in at early stages of a fire.
VERY DANGEROUS	ORANGE	61-75	No controlled buming of any nature should take place. Careful note should be taken of any sign of smoke anywhere, especially 011 the upwind side of any plantation. Any fire should be attacked with maximum force at hand. including all aircraft at the time
EXTREMELY DANGEROUS	RED	>75	All personnel and equipment should be removed from the field. Fire teams, labour and equipment are to be placed on full stand-by. At first sign of smoke, every possible measure should be taken in order to bring the free under control in the shortest possible time. All available aircraft are to be called for without delay.

Figure 2: Fire Danger Index Categories (SAWS)

Meteorological causes which have favoured the spread of fire

A first important climatic parameter in the analysis of meteorological factors that may favour the fire is the monthly rainfall deficit or excess versus annual rainfall

of a particular area. The values of this parameter are important for surface "preparation/dryness" before the fire. On April 18, the day of fire occurrence, monthly rainfall for Cape Town International Airport (Figure 3), was already below the long-term monthly average, indicating dryness.

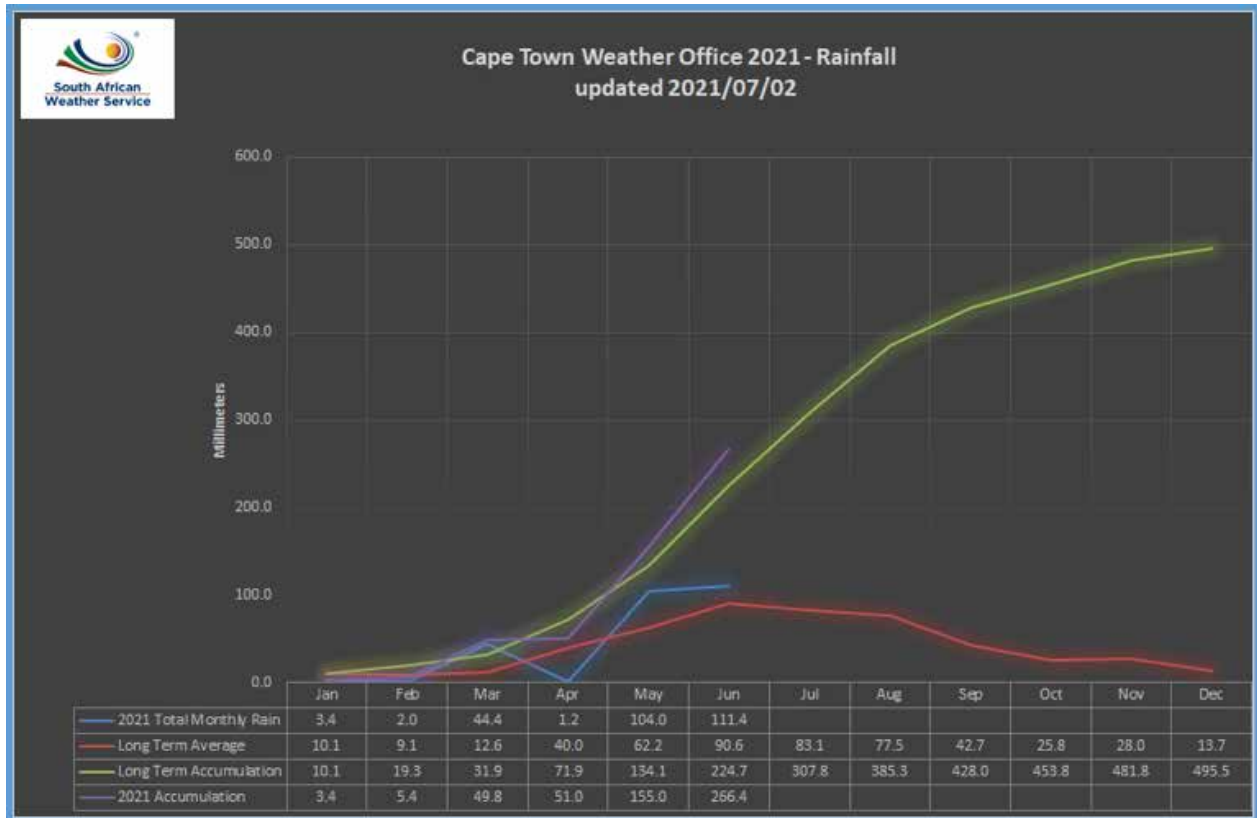


Figure 3. Total Monthly Rain v/s Long Term Average (Source: SAWS, 2021)

Another climatic parameter is the wind speed and direction. On the day of the fire occurrence, the wind at the weather stations neighbouring Table Mountain (Molteno Reservoir and Kirstenbosch) as well as at Cape Town International Airport (CTIA), was blowing at an average speed of 1.5 to 2.5 m/s (that is 5.4 to 9.0 km/h) which increased later in the day and persisted into Monday (19 April 2021). Wind gusts intensified throughout the day, reaching a speed of 8.5 m/s (or 30.6 km/h) at the Molteno Reservoir, 13.2 m/s (or 47.5 km/h) at Kirstenbosch and 14.5 m/s (or 52.2 km/h) at the CTIA.

Shown in graphical form in Figure 4 below, is the mean wind speed for 5 minutes showing the hours in which the fire occurred for the three weather stations and the time when the wind was the highest. From the graph one can see that the wind dropped around 09:00 and increased afterwards, peaking later in the afternoon at around 14:00. These wind variations persisted until the evening and there can be little doubt that any fire having started on Table Mountain, would have spread quite rapidly without very early intervention.

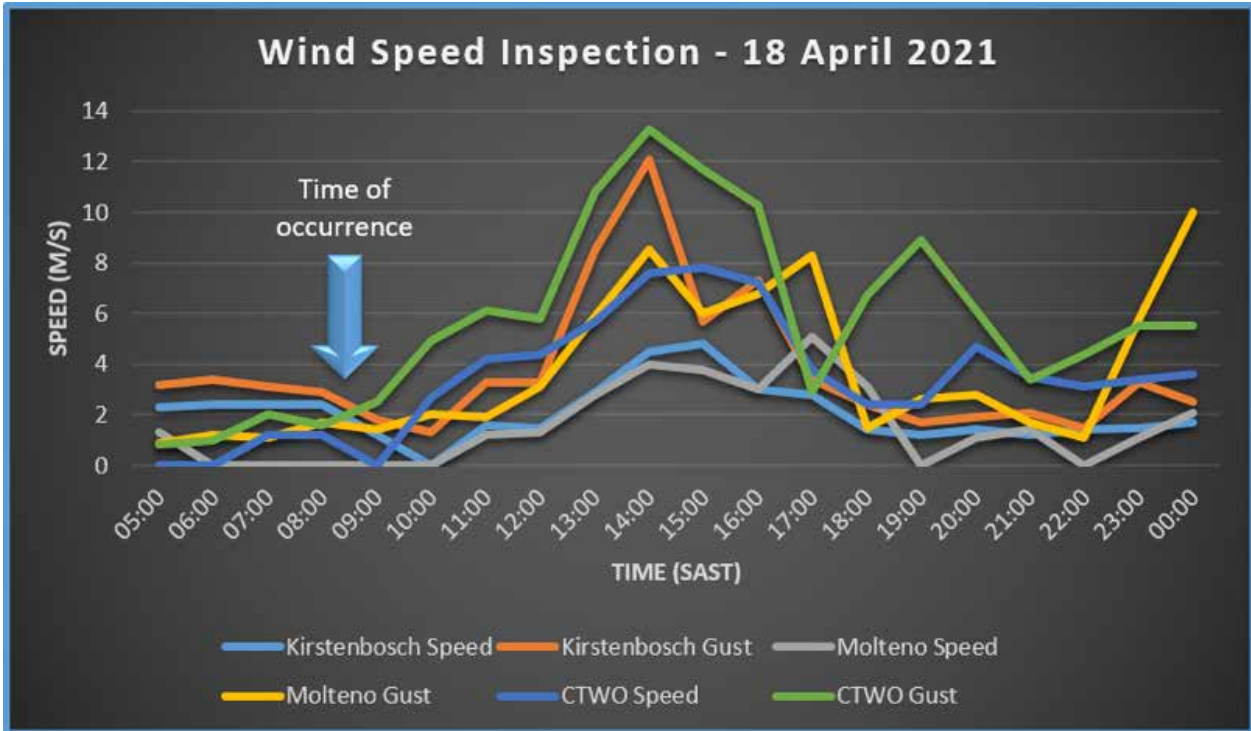


Figure 4: Wind speed between the hours in which the fire occurred. (Source: SAWS, 2021)

Tables 1-3 summarize the characteristics of meteorological variables for Molteno, Kirstenbosch and CTIA from before the fire period through to 19 April 2021. The temperature was generally warm but very hot on Sunday and cooled off on Monday (19 April 2021). There was no rainfall within the period and humidity was low to moderate. The highest average wind speed and gusts reflected for all the weather stations, occurred on the Monday. This could be one of reasons why fire-fighters battled to contain the fire because gusty conditions are very hazardous as the wind changes speed and direction rapidly.

Table 1: Meteorological Data at Molteno Reservoir, 13-19 April 2021 (SAWS, 2021)

Location	Day	Maximum Temperature (°C)	Minimum Humidity (%)	Wind speed (m/s)	Wind speed (m/s) Gusts	Precipitation (mm)
Molteno	13	32	24	0.7	2.2	0
	14	33	17	0.4	2.1	0
	15	29	26	2.4	8.1	0
	16	32	25	0.9	2.7	0
	17	21	17	0.5	1.8	0
	18	35	10	3.1	3.4	0
	19	23	58	4.1	11.3	0

Table 2: Meteorological Data at Kirstenbosch Weather Station, 13-19 April 2021 (SAWS, 2021)

Location	Day	Maximum Temperature (°C)	Minimum Humidity (%)	Wind speed (m/s)	Wind speed (m/s) Gusts	Precipitation (mm)
Kirstenbosch	13	31	31	1.2	2.6	0
	14	28	43	1.4	2.6	0
	15	21	71	2.1	4.6	0
	16	28	35	1.9	3.1	0
	17	28	42	1.5	2.5	0
	18	35	12	2.1	3.7	0
	19	18	69	2.4	5.1	0

Table 3: Meteorological Data at Cape Town International Airport, 13-19 April 2021 (SAWS, 2021)

Location	Day	Maximum Temperature (°C)	Minimum Humidity (%)	Wind speed (m/s)	Wind speed (m/s) Gusts	Precipitation (mm)
CTIA	13	32	28	2.3	4.2	0
	14	24	24	3.8	6.0	0
	15	25	48	4.9	7.8	0
	16	28	31	1.9	3.3	0
	17	29	34	0.9	2.0	0
	18	37	10	3.4	5.0	0
	19	24	47	5.6	9.0	0

Summary

Sunday, 18 April 2021 started off with light easterly wind flow which increased by late Sunday morning in and around the City of Cape Town (CoCT) Municipality. Hot and dry conditions prevailed, consequently favouring conditions for development of “runaway” fires. Gusty winds developed during Sunday afternoon and continued into Monday, 19 April 2021. These conditions hampered the firefighting efforts and the fire spread to neighbouring areas that never before had been affected by wildfires, such as the University of Cape Town.

Although a fire danger warning was not issued for any weather stations within CoCT, the fire warning was in effect across other Western Cape municipalities. Further studies on this topic are necessary in order to improve fire weather forecasts for the region and the country at large. According to the World Meteorological Organization (WMO), there is strengthened evidence

that climate change increases the frequency and/or severity of fire weather. It is on this basis that more work on fires in densely populated areas such as CoCT should be conducted.

References

- Ganteaume A., Syphard A.D. (2018) Ignition Sources. In: Manzello S. (eds) Encyclopedia of Wildfires and Wildland-Urban Interface (WUI) Fires. Springer, Cham. https://doi.org/10.1007/978-3-319-51727-8_43-1
- <https://www.readyforwildfire.org/prevent-wildfire/dead-tree-removal/>
- South African Weather Service
- Van Wilgen, B. W., 2013. Fire management in species-rich Cape fynbos shrublands. *Front Ecol Environ*, 11(1), pp. 35-44.

Pilot Operational Rip Risk Warning System

by Carla-Louise Ramjukadh

Department: Marine Unit, Cape Town Weather Office

Rip currents are important for the physical, chemical and biological circulation processes they influence in the nearshore environment (Castelle et al., 2016, Cervantes et al., 2015). However, these fast-flowing offshore currents (Figure 1) have the potential to carry unsuspecting beachgoers into deeper water (Castelle et al., 2014). The combination of exhaustion and fear causes hundreds of drownings and beach rescues (~70-80%) globally each year (Castelle et al., 2016). In the City of Cape Town, during the 2017/2018 and 2018/2019 beach-going seasons a total of 30 fatal drownings were recorded, many of which were rip current related (News24, 19 December 2019). Rip currents are currently not being operationally forecast and warned for in South Africa.



Figure 1: Rip currents indicated by the darker green water, seen at a beach near Plettenberg Bay. Source: <https://www.nsri.org.za/2020/01/beware-of-rip-currents/>

What are rip currents?

Rip currents are strong, narrow currents that extend seaward from close to the shoreline into and beyond the surf zone (MacMahan et al., 2011, Brander et al., 2016, Castelle et al., 2016). Castelle et al. (2016) identifies differentiating rip current types based on their response to varying forcing conditions, i.e. the different causes of the alongshore variations in breaking waves that are fundamental in the formation of rip currents (Figure 2). For the purpose of building an operational rip current forecast model for the South African coastline, only bathymetrically-controlled rip

current types are focused on. Bathymetrically-controlled rip currents are the most common type found on open beaches and are better understood and studied, therefore much more predictable (Scott et al., 2014, Castelle et al., 2016). Hydrodynamic processes are strongly influenced by the natural variability of beach morphology. They are the driving forces behind the relatively fixed locations of bathymetrically-controlled rip currents (Castelle et al., 2016). Under a given wave climate and tidal regime, bathymetrically-controlled rip currents vary over timescales, but importantly, are relatively persistent in space and time (Scott et al., 2014, Castelle et al., 2016).

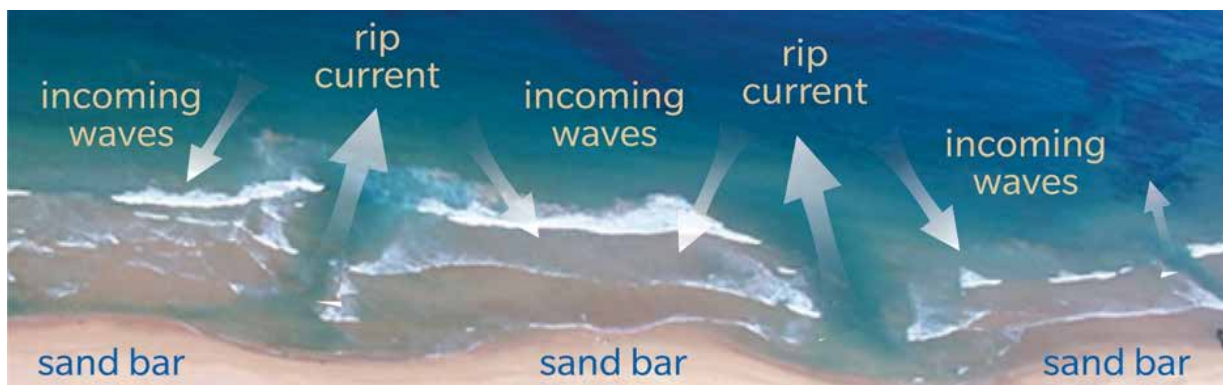


Figure 2: A schematic showing the formation and how to identify rip currents. Source: <https://beachsafe.org.au/surf-safety/ripcurrents>

The pilot operational rip risk forecast model

The Weather and Climate Science for Service Partners (WCSSPA) fund provided an exciting platform for various project partners in South Africa and the United Kingdom to build an operational rip current forecast model for the South African coastline. A collaboration between the SAWS Marine Unit and researchers from the Coastal Marine Applied Research (CMAR) group produced a pilot operational rip current risk forecast model for the Cape Peninsula. Many different components were needed to build the operational rip forecast model. These were assembled via the input and expertise of many different project partners in South Africa. Modelled inshore wave and water-level data were derived using SAWS established Wave and Storm Surge operational Table-False Bay hydrodynamic models (SWaSS and SWaSS-TM) to understand the wave and water-level conditions and identify hydrodynamic thresholds at which

rips are likely to occur. Using the SWaSS forecast model, the conditions (wave and tide) under which rip incidents have occurred were ascertained by means of a 3.5-year hindcast of waves and water-levels around the Cape Peninsula (CMAR, 2021). The high-resolution nearshore hindcast data allowed for the extraction of the wave conditions along relatively shallow depths allowing for the calculation of the theoretical significant breaking wave height required to link wave height to rip incidents (CMAR, 2021). Correlating times and dates of numerous rip incidents (data collected from beaches around the Cape Peninsula) with specific beach locations and the hydrodynamic forces occurring at that time, emerging patterns in the frequency and occurrence can be identified (CMAR, 2021). From the analysis, three levels of rip risk and an additional level for large waves were proposed (Table 1). These thresholds are a basis on which local knowledge and experience (such as those of lifeguards) can be built (CMAR, 2021).

Table 1: Table of risk levels and associated rip risk

RISK LEVEL	RIP RISK
Level 1: Low Risk	Rips Unlikely
Level 2: Medium Risk	Rips likely
Level 3: High Risk	Rips Strong
Level 4: High Wave Warning	High Waves and Strong Currents

The pilot site model is currently in the testing phase to properly ensure sufficient performance. Every day, routine hydrodynamic conditions for a 3-day forecast period are assessed against the pre-determined thresholds, generating warning flags at six different locations across the Cape Peninsula coastline (Figure 3). Numerous other outputs (Figure 4) are generated and can be neatly presented in a PDF, that will assist many different stakeholders in providing a rip risk forecast and potentially aid in beach awareness and safety.

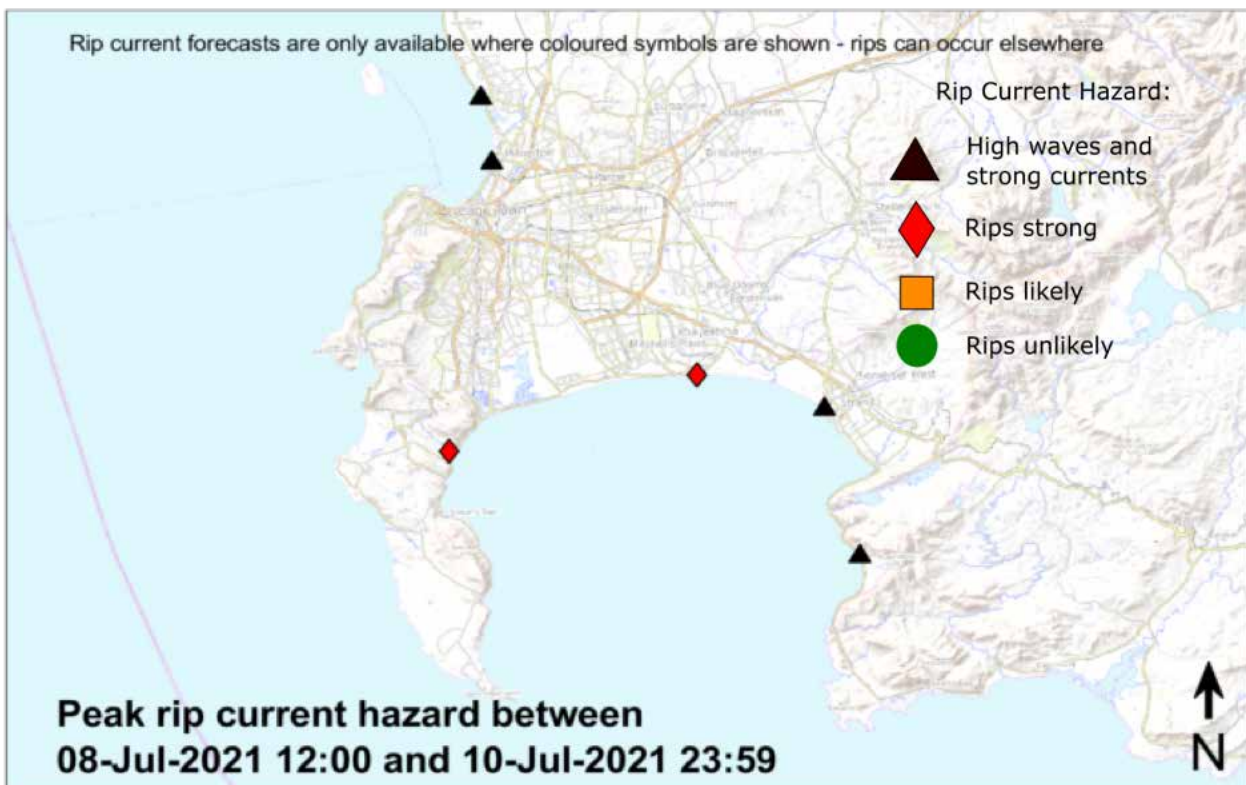


Figure 3: The rip risk forecast for 8 – 10 July 2021, for the six locations around the Cape Peninsula.

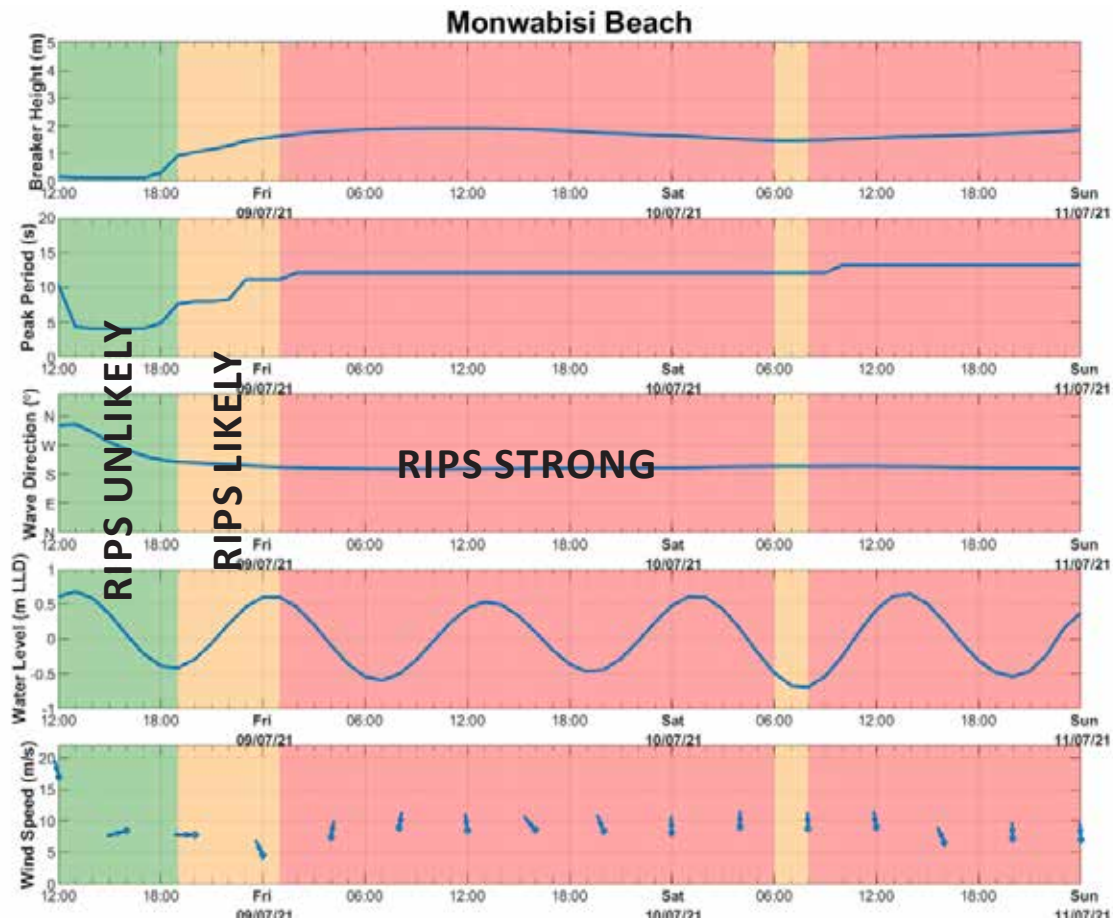


Figure 4: Time series of Monwabisi beach illustrating associated wave conditions for the forecast period 8-10 July 2021. The time series is colour-coded based on the rip risk thresholds. Rips strongly is a higher weighted rip risk level and therefore indicated as the maximum rip risk on the regional map (Figure 3).

Recently, an addendum to the standard SAWS marine IBF warning for waves was issued and re-shared by the National Sea Rescue Institute (NSRI), at their request, for the sake of public safety. The addendum mentioned that the experimental rip forecast system indicated the likelihood of strong rip currents at all six study site beaches along the Cape Peninsula. The information was received with great interest by the public and media houses, with numerous requests for more information. This bodes well for user uptake, and the reputation of SAWS in assisting to safeguard South Africans from marine weather hazards.



Figure 5: GPS drifter and dye used to study and identify rip currents in the field. Source: Rip current CMAR, presentation 2020.

Future research

The original scope of the project included the collection of in-situ field data measurements to further refine the hydrodynamic thresholds. Unfortunately, the impact of COVID-19 on this project meant that not all objectives could be met, with some being postponed. The inclusion of in-situ data will allow for the model to be better calibrated and validated. Together with the project partners, we aim to collect field measurements using GPS drifters and the release of harmless dye (Figure 5) into the rip currents, to observe their evolution. Subject to the availability of the required input data (beach profiles, incident data etc.), we aim to extend the system further around the South African coastline. A forecasting system such as this enables public safety personnel to better prepare for hazardous beach conditions (via strategic allocation of personnel and equipment, for example) and inform the public of potential danger before they head out to the beach.

Acknowledgements

Thank you to all the project partners involved: Stellenbosch University, Lifesaving SA, NSRI, the South African Weather Service (SAWS), City of Cape Town, UK Met, Council of Scientific and Industrial Research (CSIR) and most importantly the Coastal Marine Applied Research (CMAR) group at the University of Plymouth. Apologies to those not mentioned.

References

Castelle, B., Almar, R., Dorel, M., Lefebvre, J., Sénéchal, N., Anthony, E.J., Laibi, R., Chuchla, R. and de Penhoat, Y. 2014. Rip currents and circulation on a high-energy low-tide-terraced beach (Grand Popo, Benin, West Africa). *Journal of Coastal Research*. 70: 633-638.

Castelle, B., Scott, T., Brander, R.W. and McCarroll, R.J. 2016. *Earth-Science Reviews*. 163: 1-21.

Cervantes, O., Verduzco-Zapata, G., Botero, C., Olivos-Ortiz, A, Cháves Comparan, J.C. and Galicia-Pérez, M. 2015. Rip current types, circulation and hazard. *Ocean and Coastal Management*. 1-10.

Coastal Marine Applied Research, University of Plymouth Enterprise Ltd. 2021. Activity 3: Development of a pilot operational rip Hazard model. Weather and Climate Science Services Partnership (WCSSP) South Africa: Marine and Coastal Applications.

MacMahan, J., Reniers, A., Brown, J., Brander, R., Thornton, E., Staton, T., Brown, J., and Carey, W. 2011. An Introduction to Rip Currents Based on Field Observations. *Journal of Coastal Research*. 27(4) 2-4.

Scott, T., Masselink, G., Austin, M. and Russell, Paul. 2014. Controls on macrotidal rip current circulation and hazard. *Geomorphology*. 214. 198–215. 10.1016/j.geomorph.2014.02.005.

Figures:

Photograph of rip currents at a beach near Plettenberg Bay. 2020. [Photograph]. At: Plettenberg Bay: NSRI Website, News Archive.

Schematic of rip currents at a beach. Unknown. [Schematic]. At: Unknown: Surf Life Saving Website, Beach safe.

Photograph of GPS drifters. Unknown. [Photograph]. At: Unknown: CMAR 2020 Rip current presentation.

Photograph of dye released at the beach showing the rip current. Unknown. [Photograph]. At: Unknown: CMAR 2020 Rip current presentation.



Meet the Authors



Morné Gijben

Morné Gijben is a research scientist in the Nowcasting and Very Short-Range forecasting group at the South African Weather Service. He completed his BSc (Hons) degree (Meteorology) in 2010 and MSc degree (Meteorology) in 2016 on the development of a model based lightning threat index for South Africa. His fields of research include lightning, satellite, and thunderstorms in the 0 - 12 hour forecast scale. He has worked on topics like anticipating lightning activity from numerical model fields, creating a lightning climatology for South Africa with data from the South African Lightning Detection Network (SALDN), the Rapidly Developing Thunderstorm product, and various other topics related to lightning and satellite. Mr. Gijben has published several journal articles, presented papers at numerous national and international conferences, and has been involved in several externally funded projects.



Rydall Jardine

Mr Rydall B. Jardine, was born and raised in Cape Town and completed his National Diploma in Electrical Engineering at the Cape Peninsula University of Technology. He started working for the South African Weather Service in January 1998. He also holds a bachelor's in electrical engineering through Tshwane University of Technology. He has over 20 years of experience within the Meteorological Infrastructure maintenance working on weather radars, high frequency transmitters, lightning detection infrastructure, manual and automated weather systems, as well as aviation weather observation and monitoring infrastructure.

He was tasked by the South African Weather Service to lead the deployment of Automated Weather Systems into the larger African Continent, where he ensured the successful deployment into Tanzania, Swaziland, Lesotho, Namibia and Zambia. He is currently the Manager: Infrastructure Availability within the company overseeing the Radar and Lightning Detection Networks; and is currently also fully the role of Acting Senior Manager: Technical Service overseeing all the company's weather observation infrastructure supported by a team of technicians, technologist, specialist and engineers.



Nompumelelo Kleinboo

Nompumelelo Kleinboo is a forecaster currently based at the Port Elizabeth (Gqeberha) Weather Office. She completed her BSc (undergraduate) and honours degrees in Meteorology at the University of Pretoria in 2015 and 2016 respectively. In 2017, she then completed the SAWS forecasting internship programme offered by the Regional Training Centre (RTC).

She enjoys engaging different stakeholders, especially aviation clients. Apart from weather forecasting, she also has interests in the climate variability of South Africa.





Dr Andries Kruger

Dr Andries Kruger is a Chief Scientist: Climate Data Analysis and Research in the Department: Climate Service of the South African Weather Service. His present and previous duties include the creation and writing of general climate publications, climate change and variability research with historical data as input, ad hoc scientific projects of which the numbers have increased substantially in recent years, climate data and information requests, where advanced statistical analyses are required, drought monitoring, and assisting in the quality control of climate data.

In 2001, Dr Kruger obtained a PhD (Civil Engineering) degree at the University of Stellenbosch on the research topic “Wind Climatology and Statistics of South Africa relevant to the Design of the Build Environment”. Before that, he obtained an MSc (Environmental and Geographical Science) degree at the University of Cape Town. He has published papers both locally and internationally, and authored a SAWS series of publications on the general climate of South Africa. He is widely recognised, both nationally and internationally, for his research, which involves advanced statistical analyses and interpretation of historical climate data.



Brighton Mabasa

Mr. Brighton Mabasa is a research scientist in Applications (Renewable Energy Applications and scientific consulting) at South African Weather Service (SAWS). Brighton's duties in the group includes SAWS Solar Radiometric Network monitoring and maintenance, data archiving, data quality control using Baseline Solar Radiation Network (BSRN) standards, satellite data validation, product development, observation data preparation for model verification, solar radiation and biometeorology station installation and calibration using ISO standards, writing peer reviewed articles and writing Standard Operating Procedures (SOPs) for operational activities.

Brighton Mabasa is registering for MSc in Atmospheric Physics at UNISA, research outputs will support an advanced operation of the SAWS solar radiometric network.



Stella Nake

Ms Stella Nake was born in a village approximately 100km outside of Pretoria, called Ratjiepan. The indigenous weather knowledge from the community fascinated her so much, and she undoubtedly picked up an interest in weather forecasting at a very early age. She can remember as a young girl, sitting under a tree watching the clouds as they move over ahead of a thunderstorm; and she asked herself: “who was pushing the clouds and where did lightning come from?”

When she was in Grade 12, a group of students from the Department of Geography, Geophysics and Meteorology of the University of Pretoria visited their school as part of their school outreach programme. They showed the learners weather observing instruments and explained to them what weather forecasting was all about. She got inspired and a year later after matric enrolled at the University of Pretoria as a Meteorology student! After completing her Honours Degree in Meteorology in 2006, she joined SAWS as a Weather Forecaster based at Cape Town Weather Office until the present.





Carla-Louise Ramjukadh

Carla-Louise Ramjukadh, is a Scientist, working and contributing to various exciting advances and products within the SAWS Marine Unit, based at the Cape Town Weather Office. Currently her focus lies with coastal vulnerability and hazards, along our South African coastline



Dr. Henerica Tazvinga

Dr. Henerica Tazvinga is a lead scientist for Energy at the South African Weather Service (SAWS). She has a PhD (Engineering) from University of Pretoria and Msc in Renewable Energy. Henerica has wide experience in renewable energy systems, energy efficiency and engineering acquired over 25 years having worked as a lecture, researcher and engineer in educational, technological and industrial institutions.

Her research interests are in energy optimization and management of micro-grid systems, and meteorology for energy sector. She has participated in many local and international energy projects. Further to this, Dr. Henerica Tazvinga received the National Research Foundation Scare Skills Award in 2014 and UK Newton Fund Award in collaborations with the University of Strathclyde in 2016 (Electric vehicle study).

Prior to joining SAWS, she worked for organisations such as CSIR as a Hybrid Power Plant Specialist and the University of Pretoria's Energy efficiency and demand side Management Hub & Centre of New Energy Systems as a senior Management and Verification engineer. She also worked as a lecture at Polytechnics and Universities where

she taught in Production, Mechanotrics and Fuels and energy Engineering Departments.

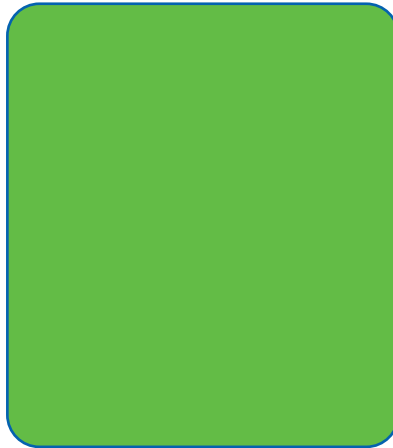
She is a member of organisations such as the Southern African Research & Innovation Management Association (SARIMA); Southern African Solar Thermal Training (SOLTRAIN); International Solar Energy Society, Global Women's Network for the Energy Transition (GWNET) and institute of Electrical and Electronics Engineers (IEEE). Dr.Tazvinga has published many articles on hybrid energy systems and is a reviewer of many high impact energy journals including Applied Energy , Solar Energy, IEEE Access and IET Generation, Transmission & Distribution ; Energy Policy, International Journal of Electrical Power and Energy Systems, Energy Strategy Reviews as well as the Journal in Southern Africa (JESA) .She is a National Research Foundation rated researcher. Dr. Henerica also serves as an Evaluator and Assessor for the National Research Foundation Engineering Panel and has served on several international local technical advisory, organising and review for committees for conferences. She also supervises students and has served as an external examiner for several local universities.



Ayabonga Tshungwana

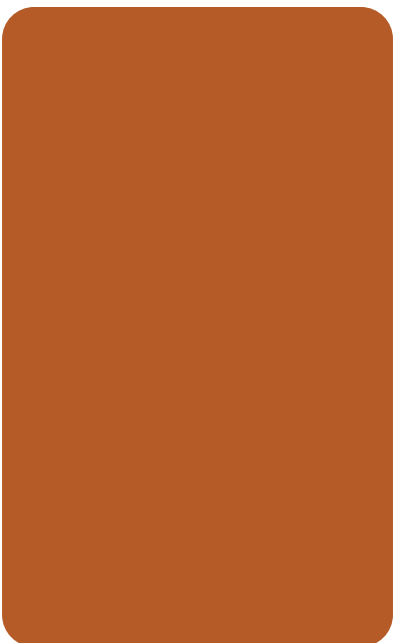
Ayabonga Tshungwana obtained his first BSc degree at University of Fort Hare majoring with Physics, Maths and Applied Maths (2016).

He then obtained his BSc Meteorology at University of Pretoria through a programme called "Bridging course (2017)" and obtained his BSc Honours in Meteorology at University of Pretoria (2018). He completed the forecasting certificate at South African Weather Service (2019).



Nosipho Zwane

Ms Nisipho Zwane is a research scientist at the South African Weather Service since 2014. She began specialising in Climate Change and recently moved to Application Research under the Energy Unit. She completed her BSc degree with a double major in Environmental and Geographical Science and Ocean and Atmosphere Science in 2012 (University of Cape Town). In 2013 she completed her BSc Honours in Ocean and Atmosphere Science (University of Cape Town). She is currently enrolled for MSc Meteorology at the University of Pretoria.



Head Office

Centurion

Eco Glades
Block 1B, Eco Park
Cnr Olievenhoutbosch and
Ribbon Grass Streets
Centurion
0157

Regional Offices

Bloemfontein

Weather Office
Maselspoort Road
Bram Fisher International Airport
Private Bag X20562
Bloemfontein
9300
Tel: 051 433 3281

Cape Town International

Weather Office
ATNS Tower
Tower Street
Cape Town International Airport
PO Box 21
Cape Town International Airport
7525
Tel: 021 934 0749/0831

King Shaka International

Weather Office
Ground Floor
ATNS Building
King Shaka International Airport
PO Box 57733
King Shaka International Airport
4407
Tel: 032 436 3820/3812

OR Tambo International

Aviation Weather Centre
Room N161
3rd Floor
OR Tambo International Airport
PO Box 1194
Kempton Park
1627
Tel: 011 390 9329/9330

Port Elizabeth

Weather Office
Roof Top
Departures Hall
Port Elizabeth Airport
Private Bag X5991
Walmer
Port Elizabeth
6065
Tel: 041 581 0403/8587

WEATHERSMART NEWS

Scientific meteorological and climatological
news from the South Africa Weather Service



**South African
Weather Service**

